Palestine Polytechnic University

College of Engineering & Technology

Mechanical Engineering Department

Simulation and Analysis of a Vehicle Chassis by ANSYS Program

Project Team:

Taqi Aldeen Abo Al-kibash

Mohammad Hasan

Supervisor:

Dr. Hussein Amro

Submitted to the College of Engineering
In partial fulfillment of the requirements for the
Bachelor degree in Automotive Engineering

May, 2019

Palestine Polytechnic University
College of Engineering & Technology
Mechanical Engineering Department

Simulation and Analysis of a Vehicle Chassis by ANSYS Program

Project Team:
Taqi Aldeen Abo Al-kibash
Mohammad Hasan

Submitted to the College of Engineering
In partial fulfillment of the requirements for the
Bachelor degree in Automotive Engineering

Supervisor signature:

Dr. Hussein Amro

.....

Department head signature:

Dr. Iyad Hashlamon

.....

May, 2019

Table of Content

List of Tables V
List of Figures V
Dedication VII
Acknowledgment VIII
Abstract IX

Chapter One : Project Introduction 1

1.1 Overview 2
1.2 Problem Definition 2
1.3 Project Contribution 3
1.4 Motivations 3
1.5 Project Objectives 3
1.6 Project Challenge 4
1.7 Literature Review 4
1.8 Methodology Overview 6
1.9 Project Action Plan 6

Chapter Two : Project Analysis Methodology and Mathematics 8

2.1 Short History 9
2.2 Engineering Problems 9
2.3 Numerical Methods 10
2.4 Basic ANSYS Structure 10
2.5 Explicit Dynamics Analysis System 13
2.5.1 Explicit Dynamics Applications 13
2.5.2 System Solving Strategy 13
2.5.3 Explicit Transient Dynamics 14
2.5.4 Explicit Time Integration 16
2.6 Verification of Results 17
2.7 Impulse Momentum and Impact 18
2.7.1 Linear Impulse and Linear Momentum 18
2.7.1.1 For Particles 18
2.7.1.2 For System of Particles 21
2.7.1.3 For Rigid Bodies 22

2.7.2 Impacts of Particles 24
2.7.2.1 Direct Central Impact 24
2.7.2.2 Coefficient of Restitution 25
2.7.3 Impacts of Rigid Bodies 26
2.8 Stress and Strain Analysis 26
2.8.1 Stress and Strain Definition 26
2.8.2 Stress-Strain Diagram 29
2.8.3 Elasticity and Plasticity Behavior of Materials 31
2.8.4 Hooke's Law and Poisson's Ratio Definition 33
2.8.5 Strain Energy Principle 36

Chapter Three : Project Modeling Design and Results Clarification 40

3.1 Introduction 41
3.2 Design Description 41
3.2.1 Design Overview 41
3.2.2 Models Description 44
3.3 Simulation Methodology 46
3.4 Results Clarification 53
3.4.1 Simulation Results 53
3.4.2 Results Discussion 56

Chapter Four : Project Conclusion and Recommendations 58

4.1 Project General Conclusion 59
4.2 Recommendations 60

References 61

List of Tables

Table 1.1: Distribution of tasks on the first and second semesters 7
Table 3.1: Chassis and Wall material characteristic 48

List of Figures

Figure 2.1: ANSYS (R17.0) Graphical User Interface (GUI) 11
Figure 2.2: Explicit dynamics solution algorithm 14
Figure 2.3: General curvilinear motion in space of a particle of mass (m) 18
Figure 2.4: Impulse-Momentum diagram 20
Figure 2.5: Force-Time diagram 21
Figure 2.6: Representative particle of mass $\boldsymbol{m_i}$ 22
Figure 2.7: Collinear motion and impacts of two spheres 24
Figure 2.8: Prismatic bar in tension 27
Figure 2.9: Stress-strain diagram for a typical structural steel in tension 30
Figure 2.10: Stress-Strain diagrams illustrating elastic behavior, and partially elastic behavior ... 32
Figure 2.11: Axial elongation and lateral contraction of a prismatic bar in tension 34
Figure 2.12: Prismatic bar subjected to a statically applied load 36
Figure 2.13: Load-displacement diagram 37
Figure 2.14: Elastic and inelastic strain energy 38

Figure 3.1: Defender's chassis 41
Figure 3.2: "A-model" design 42
Figure 3.3: "B-model" design 43
Figure 3.4: "C-model" design 43
Figure 3.5: The sketch of the main bridge longitudinal-section 44
Figure 3.6: The cross-sectional sketch for cross-bridges 45
Figure 3.7: The Rear bumper sketch 45
Figure 3.8: Defender chassis characteristics information 45
Figure3.9: Frontal impact test description 46
Figure 3.10: Chassis to the concrete wall view 46
Figure 3.11: ANSYS program interface 47
Figure 3.12: Toolbox and project schematic interface 47
Figure 3.13: Engineering data interface 48
Figure 3.14: The modeling files importing methods 49

Figure 3.15: The wall sketch with geometrical dimensions 49
Figure 3.16: The concrete wall with its cross-sectional sketch 50
Figure 3.17: Discretization process with the meshing shape on the model 50
Figure 3.18: The back face of the wall as a static fixed support 51
Figure 3.19: The chassis velocity determination 51
Figure 3.20: The inserting method of the solution process results 52
Figure 3.21: The common results observation point determination 52
Figure 3.22: The sampling result of stress for the "A-model" design 53
Figure 3.23: Total deflection values for three models due to increasing of speed 54
Figure 3.24: Equivalent von-mises stress values for three models due to increasing of speed . . 55
Figure 3.25: The stress-strain curves for the three models at the observation point 56

Dedication

To our great Palestine …… The cradle of prophets and the land of messages

To our holy Jerusalem …... The eternal capital of Palestine

To our righteous martyrs … Who gave their lives as honor to their country

To our brave prisoners …... Who preferred dignity to humiliation

To our Virtuous teachers … Who supported us until the end

To our first teacher …… Our Prophet Muhammad (*peace be upon to him*)

To our supervisors ……. Especially Dr. Hussein Amro

To our families …….. For all that they have given us throughout our lives

To our friends ……... Who shared us our moments of gladness and sadness

To our second family …. The Department of Mechanical Engineering , *PPU*

To everyone who shared us the hope until the end

We present you our graduation project, which is the result of our scientific achievement for the years we spent together.

Our respect and appreciation to all of you

Taqi Aldeen Abo Al-kibash

Mohammad Hasan

Acknowledgment

This project was not carried out without the help and support that all of you are giving to us, we thank you very much for that. The first to start thanking him is the God - *the Almighty* -, where that all thanks at the first and at the last are only for the God -*the Almighty* -, with no partner of that.

Then, we thank all those who helped us from the academic staff in the Department of Mechanical Engineering, especially our supervisors: Dr. Hussein Amro, Dr. Majdi Zalloum, and Dr. Yousef Sweiti, who were giving us all advices that we need at the studying of the subject of this project.

Finally, we thank all those who participated in the success of this project and did not mention their names here, but our hearts keep thanks and gratitude to them, especially our families.

Thank you very much

Taqi Aldeen Abo Al-kibash

Abstract

Automotive chassis, is the most important part of an automobile. The chassis serves as a framework for supporting the body and different parts of the vehicle, so it should be rigid enough to withstand the shock, twist, vibration and other stresses. Therefore, there are many criteria that must be taken into consideration when designing a chassis structure, where some of these criteria are what the manufacturers lay out for themselves when determining the characteristics of the chassis, and others criteria was based on the engineering design principles. As a result, strength and stiffness are two important criteria for the design of the chassis. Also, the weight of the chassis is an important consideration in chassis design due to its direct relationship with the amount of fuel consumption and the emissions rates, which emitted to the surrounding atmosphere. This project analyzing the structural design of a specific vehicle chassis by using the theory of finite element method (FEM), which performed by simulating the chassis model into a frontal car crash tests using ANSYS Workbench program. This project aims to achieve analytical results that will be recommended into a the next chassis design criteria, where it turns out that the cross-bridges, that the structure consist of, have a major role in mitigating the effect of the collision on the rest of the body of the vehicle.

الملخص

هيكل المركبة ، أهم أجزاء السيارة و أساس بنائها ، حيث يمثل الهيكل إطارا لدعم جسم السيارة و مكوناتها الأخرى ، لذلك يجب أن يكون قويا بما يكفي لتحمل الصدمات ، و الالتواءات ، والاهتزازات وغيرها من القوى التي سيتعرض لها كجزء أساسي في المركبة . هنالك العديد من المعايير التصميمية التي يجب أن تأخذ بعين الاعتبار عند تصميم هيكل المركبة ، والتي تتمثل فيما يضعه المصنعون لأنفسهم من خصائص للهيكل ، تعتمد على مميزات السيارة ، و حجمها ، و وظيفتها ، في حين تستند معايير أخرى إلى مبادئ التصميم الهندسي وأسسه وقوانينه . نتيجة لذلك ، تعتبر القوة والصلابة أحد أهم المعايير التصميمية للهيكل ، كما يعتبر وزن الهيكل أيضا أحد أهم محددات التصميم ، نظر ا لعلاقته المباشرة بكمية استهلاك الوقود ونسب الانبعاثات المنبعثة من المركبة إلى الغلاف الجوي . يقوم هذا المشروع بتحليل التصميم الهيكلي لهيكل مركبة معينة باستخدام نظرية العناصر المحدودة (FEM) ، وذلك من خلال إخضاع نموذج تصميمي للهيكل ضمن مجموعة من عمليات محاكاة اختبارات التصادم الأمامية للسيارات ، باستخدام برنامج التحليل الهندسي المحوسب (ANSYS) . يهدف المشروع بذلك إلى تحقيق نتائج هندسية تحليلية لبنية الهيكل ، تستخدم فيما بعد كتوصيات هندسية يستعان بها عند استحداث تصاميم جديدة للهيكل في المستقبل ، حيث اتضح أن الجسور العرضية- التي يتكون منها الهيكل - لها دور رئيسي في التخفيف من تأثير التصادم على بقية جسم السيارة.

1

Chapter One

Project Introduction

1.1 Overview.
1.2 Problem Definition.
1.3 Project Contribution.
1.4 Motivations.
1.5 Project Objectives.
1.6 Project Challenge.
1.7 Literature Review.
1.8 Methodology Overview.
1.9 Project Action Plan.

1.1 Overview

In 1886, the first real appearance of a car powered by an internal combustion engine, by the German engineer Carl Benz, was not intended to exceed the principle of applying the theory of a vehicle that operates with the gasoline as a fuel. Then, the vehicles were developed in parallel with the great industrial revolutions development in the twentieth century, where the forms, sizes and functions of the vehicles were developed to serve the needs of society and meet the wishes of customers. The automotive industry has a great development, significantly in recent decades, after the using of simulation and design analysis programs for the different parts of the vehicle in multiple working conditions, which provided a lot of effort and time in the processes of manufacturing and developing the vehicles.

In the recent period of the industrial history, the automotive industry is facing many challenges, due to the existence of environmental challenges and international laws, which aims to preserving the environment in terms of natural resources that are nearing to extinction and due to the negative environmental phenomena such as global warming. There are many areas of development in the automotive industry that aimed to achieve and apply environmental laws. The main goal is to reduction the use of fossil fuels or to obtain a renewable, sustainable and alternative energy sources, as well as to mitigate emissions from vehicles.

This scientific research aims to study one aspect of development of the automotive industry by focusing the study on a specific part of the car. The development of this part is a general development of the automotive industry, because is a common part in all vehicles. This research is based on the studying of the main vehicles structure (vehicle chassis), by taking a specific model and subjecting it on a scientific simulation and analysis programs to identify all the characteristics of this model such as static and dynamic characteristics, especially the ANSYS program which will be use in this study.

The development of vehicle structures aims to get the best utilization of the available environmental materials in manufacturing processes to achieve a greater chassis durability and a best quality, as well as obtaining a lighter chassis weight provides a greater energy and reduces the amount of emissions emitted to the surrounding atmosphere, due to the reduction of vehicle inertia which depending in the weight of the vehicle and its components.

1.2 Problem Definition

The scarcity of environmental resources and the climate changes in the modern world has prompted countries to create legislation and laws to limit this phenomenon to all industrial sectors that causes or participates that. The automotive sector is one of these sectors whose production of

vehicles has become restricted by international environmental laws and standards such as the European Environment Agency (EEA).

1.3 Project Contribution

This project is a scientific research on the durability of the vehicle chassis structure and its rigidity during accidents, especially the frontal collision, where the project looks at the characteristics of the real chassis structure of a vehicle of Land Rover by studying its physical characteristics after the collision and compares these qualities between three different models for this vehicle structure. This research presents a model of the chassis structure where showing its dimensions and general shape, which are kept as a company's secrets. The research also presents analytical results for the collision of this structure with another body, which are the basis for the development hypotheses later.

1.4 Motivations

Manufacturing and development in the automotive industry is a secret that no one can see, while the products are presented as a competitive tool between these industrial companies. As a result of being an automotive engineer, we are concerned in the design of vehicles and its structures. Knowing the secrets of this industry is the main motivation for this research, to know the vehicle designs secrets. It is also our turn to understand these designs and build similar ones to offer the community a better level of safety for passengers, and lower levels of energy consumption and emissions.

1.5 Project Objectives

The main objectives of the project are to Analyze a durability of a vehicle chassis by subjecting it to a collision events, where these results will be used to obtain a suitable design for a particular vehicle structure that takes in consideration the environmental laws. Also, there is a sub objective for the project, which is the learning on one of the most important engineering analysis programs and the most common, the ANSYS program, as well as the learning of the design techniques and their principals.

1.6 Project Challenge

The extreme competition between the car manufacturers is one of the obstacles that stand in the way of applying this research because these companies aims to produce a vehicle with the best specifications, which makes any information in this framework one of a company's top secrets, that can't be revealed, so that will make the information collection process to study or development is too difficult process. Therefore, finding a real model is very difficult and can't be achieved. As a result, finding a model that describes the chassis structure for the vehicle that will be considered, in this research, is one of the biggest challenges in the project.

Also, there is another challenge in this project, which is the learning on the engineering analysis program (ANSYS) without any courses or tutorial in this subject. Therefore, a personal learning in this case is the solution, but to have all the needed knowledge with all specified details required to achieve this project personally is considered a challenge itself.

1.7 Literature Review

Patel Vijaykumar and others [1] focused their work towards weight reduction of chassis by performing structural analysis. Basic calculations for the chassis frame were done systematically based on the bending theory and values of stress and deflection was obtained. Finite element analysis for the existing chassis was performed for overload condition and stress and deflection values were received. For weight reduction, design modifications were made by doing a sensitivity analysis. In a sensitivity analysis, part modulus and flange width were kept constant. Three cases were considered for weight reduction in which thickness and height of the flange were diverse. Comparison of the results showed that out of three cases the third case resulted in a weight reduction of about 7% and stress and deflection values were reduced by about 12% and 11% respectively.

S. S. Sane and others [2] performed stress analysis of a light commercial vehicle chassis by using finite element method. Initially analysis of the actual chassis of the vehicle was performed and values of the stress and deflection were gathered. A total of nine different load cases were considered for the analysis of the chassis. To reduce the stress values stiffeners of changing height were added at the critical locations. The chassis was analyzed by finite element method using Altair Hyper Works software package. Identification of the results showed that stresses at the critical location were reduced up to 44% by addition of stiffener.

Marco Cavazzuti and others [3] focused their study on weight reduction of the automotive chassis by using structural optimization method linked with finite element analysis. Various optimization techniques were explained. The methods were briefly introduced, and some applications were

presented and discussed with the aim of showing their potential. A particular focus was given to weight reduction in automotive chassis design applications. The author provided a quick overview of structural optimization methods. The author explained how topology and topometry optimizations were more convenient for an early development stage, whose outcome could be further refined through size and shape optimizations.

Ravi Chandra and others [4], described the analysis of heavy vehicle chassis for weight reduction using PRO–E software for designing, ANSYS 12.0 for analysis. The dimensions of the heavy vehicle chassis of a TATA 2515EX vehicle was taken for modeling and analysis of a heavy vehicle chassis among three different composite materials namely, Carbon/Epoxy, E-glass/Epoxy, and S-glass /Epoxy subjected to the equal pressure as that of a steel chassis. The design constraints were stresses and deflections. The three various composite heavy vehicle chassis have been modeled by considering three various cross-sections. Namely, C, I and Box type cross sections. For validation, the design was done by applying the vertical loads acting on the horizontal various cross sections. From the results, it was observed that the polymeric composite heavy vehicle chassis is lighter and more practical than the conventional steel chassis with similar design specifications.

Hemant Patil and others [5] presented stress analysis of a ladder type low loader truck chassis structure consisting of C-beams design using CATIA V5R10 and ANSYS. In order to achieve a reduction in the magnitude of stress at the critical point of the chassis frame, side member thickness, cross member thickness and position of a cross member from rear end were varied. Numerical results showed that if the thickness change is not possible, changing the location of cross member may be a good alternative. Computed results were compared to analytical calculation, where it was constructed that the maximum deflection agrees well with theoretical approximation but varies on the magnitude aspect. They concluded that it is better to change the thickness of cross member at critical stress point than changing the thickness of side member and position of chassis for a reduction in stress values and deflection of chassis.

Hirak Patel and others [6], presented an analysis of the static stress that acting on the upper surface of the truck chassis. Critical parts that will heavy to failure were also observed. 3-D finite element model of the truck chassis was made using Pro-E before analyzed through ANSYS software. Model updating of truck chassis model was prepared to adjust the selective plots such as mass density and Poisson’s ratio. Numerical results showed that critical part was at the arise joint of the tire and also at the front part of the chassis. Some modifications were also suggested to reduce the stress and to increase the strength of the truck chassis.

Madan Mohan Reddy and others [7] investigated the modeling and analysis of container chassis using FEM to improve load bearing capacity and reducing the failure of chassis with bending by adding stiffeners. The rectangular stiffeners to be placed in between the cross affiliates and fastened to chassis by means of bolts. The analysis results of Ansys-14 display that there is a reduction in von misses stress in chassis with stiffener up to the extent of 37.11% compared to without stiffener while stress magnitude reduced up to 36.23% and deflection reduced by 36.16%.

Swami K.I and others [8] investigated the static structural analysis of truck chassis with the help of ANSYS software. Here the chassis of Eicher 20.16 is of ladder frame category which has two side affiliates or longitudinal members of C- cross section and seven transverse division called cross members of C- cross section. The results from graph show that as the side affiliate thickness increases, initially there is a slight decrease in the maximum value of von misses stress but afterward, it starts increasing. The rate decreases in just before the end and again increases at the end.

1.8 Methodology Overview

To achieve the objectives of the project, the methodology will begin with a model creation, which represent the identified vehicle chassis in this project. Then, it will be subjected into a range of engineering analyzes process, which based on the simulation of one of the car crash tests and then collecting the analytical results to represent it in this project. Chapter three illustrates the methodology and detailed steps of the project framework.

1.9 Project Action Plan

The project selection, formulation its ideas, identification a good previous studies and the collection for a basic information to starting up in the project were the most important tasks carried out at the first semester. Also, determining the type of the vehicle that will be examined at the project and start collecting information about it, as well as the learning on the ANSYS program are one of the most important tasks that began at the first semester.

The chassis structure drawing with its three models by the CATIA program, inserting them into the ANSYS program, applying the principle of collisions simulation, dealing with the processes problems, information collection, and writing the final report were the most important tasks carried out during the second semester. Table (1.1) shows the distribution of tasks on the first and second semesters over a period of (16) weeks for each.

Table 1.1: Distribution of tasks on the first and second semesters.

Tasks per weeks	First semester weeks															
	1	2	3	4	5	6	7	8	9	10	11	12	13	14	15	16
Project selection																
Information collection																
Literature review studying																
Learning on (ANSYS) software																
Finding a research model																
Writing the first semester report																
Tasks per weeks	**Second semester weeks**															
	1	2	3	4	5	6	7	8	9	10	11	12	13	14	15	16
Chassis structure drawing																
Connect two programs together																
Solving the modeling problems																
Simulating the crash tests																
Information collection																
Writing the final report																

2

Chapter Two

Project Analysis Methodology and Mathematics

2.1 Short History.
2.2 Engineering Problems.
2.3 Numerical Methods.
2.4 Basic ANSYS Structure.
2.5 Explicit Dynamics Analysis System.
2.5.1 Explicit Dynamics Applications.
2.5.2 System Solving Strategy.
2.5.3 Explicit Transient Dynamics.
2.5.4 Explicit Time Integration.
2.6 Verification of Results.
2.7 Impulse Momentum and Impact.
2.7.1 Linear Impulse and Linear Momentum.
2.7.1.1 For Particles.
2.7.1.2 For System of Particles.
2.7.1.3 For Rigid Bodies.
2.7.2 Impacts of Particles.
2.7.2.1 Direct Central Impact.
2.7.2.2 Coefficient of Restitution.
2.7.3 Impacts of Rigid Bodies.
2.8 Stress and Strain Analysis.
2.8.1 Stress and Strain Definition.
2.8.2 Stress-Strain Diagram.
2.8.3 Elasticity and Plasticity Behavior of Materials.
2.8.4 Hooke's Law and Poisson's Ratio Definition.
2.8.5 Strain Energy Principle.

2.1 Short History

The usage of the Finite Element Method as a tool to solve engineering problems commercially in industrial applications is quite new. It was used in the late 1950's and early 60's, but not in the same way as it is today. In the mid 60's, very specialized computer programs were used to perform the analysis. The 1970's was the time when commercial programs started to emerge. At first, FEM was limited to expensive mainframe computers owned by the aeronautics, automotive, defense and nuclear industries. However, in the late 70's more companies started to use the FEM, and since then, the usage has grown very rapidly.

Today commercial programs are large and very powerful, complex problems can be solved by one person on a PC. Many of them have the ability to handle different kinds of physical phenomena such as thermo mechanics, electro mechanics and structural mechanics. One often talks about multi physics, where different kinds of physical phenomena are coupled in the same analysis. There are many available commercial programs, ABAQUS, FLUENT, Comsol Multiphysics, and ANSYS are just a few examples. A full license of a finite element analysis program usually cost on the order of several tens of thousands of Euros. ANSYS is a widely used commercial general-purpose finite element analysis program.

2.2 Engineering Problems

In general, engineering problems are mathematical models of physical situations. Mathematical models are differential equations with a set of corresponding boundary and initial conditions. The differential equations are derived by applying the fundamental laws and principles of nature to a system or a control volume. These governing equations represent balance of mass, force, or energy. When possible, the exact solution of these equations renders detailed behavior of a system under a given set of conditions.

The analytical solutions are composed of two parts: a homogenous part, and a particular part. In any given engineering problem, there are two sets of parameters that influence the way in which a system behaves: parameters that provide information regarding the natural behavior of a given system. These parameters include properties such as modulus of elasticity, thermal conductivity, and viscosity. On the other hand, there are parameters that produce disturbances in a system. These parameters include external forces, moments, temperature difference across a medium, and pressure difference in fluid flow.

2.3 Numerical Methods

There are many practical engineering problems for which we cannot obtain exact solutions. This inability to obtain an exact solution may be attributed to either the complex nature of governing differential equations or the difficulties that arise from dealing with the boundary and initial conditions. To deal with such problems, we resort to numerical approximations In contrast to analytical solutions, which show the exact behavior of a system at any point within the system, numerical solutions approximate exact solutions only at discrete points called nodes, which is the first step of any numerical procedure. This process divides the desired medium into a number of small sub regions and nodes There are two common classes of numerical methods: Finite Difference Methods (FDM), and Finite Element Methods (FEM).

With finite difference methods, the differential equation is written for each node, and the derivatives are replaced by difference equations. This approach results in a set of simultaneous linear equations. Although finite difference methods are easy to understand and employ in simple problems, but they are become difficult to apply on problems with complex geometry or complex boundary conditions, this situation is also true for problems with non-isotropic material properties.

In contrast, the finite element method uses integral formulations rather than difference equations to create a system of algebraic equations. Moreover, an approximate continuous function is assumed to represent the solution for each element. The complete solution is then generated by connecting or assembling the individual solutions, allowing for continuity at the inter elemental boundaries. As a result, the finite element method(FEM) is a numerical procedure that can be applied to obtain solutions to a variety of problems in engineering science. Steady, transient, linear, or nonlinear problems in stress analysis, heat transfer, fluid flow, and electromagnetism problems.

2.4 Basic ANSYS Structure

ANSYS is a comprehensive general-purpose finite element computer program, which capable of performing static, dynamic, heat transfer, fluid flow, and electromagnetism analyses. The current version of ANSYS has a completely new look, with multiple windows incorporating Graphical User Interface (GUI), utility menu, input window, and a toolbar. Today, you will find ANSYS in use in many engineering fields, including aerospace, automotive, and electronics because the ANSYS is a very powerful and impressive engineering tool that may be used to solve a variety of problems.

Treatment of engineering problems generally contains three main parts: create a model, solve the problem, analyze the results. ANSYS, like many other FE-programs, is also divided into three main parts (processors) which are called preprocessor, solution processor, postprocessor. Other software may contain only the preprocessing part or only the post processing part. During the analysis you will communicate with ANSYS via a Graphical User Interface (GUI), which seen in figure (2.1).

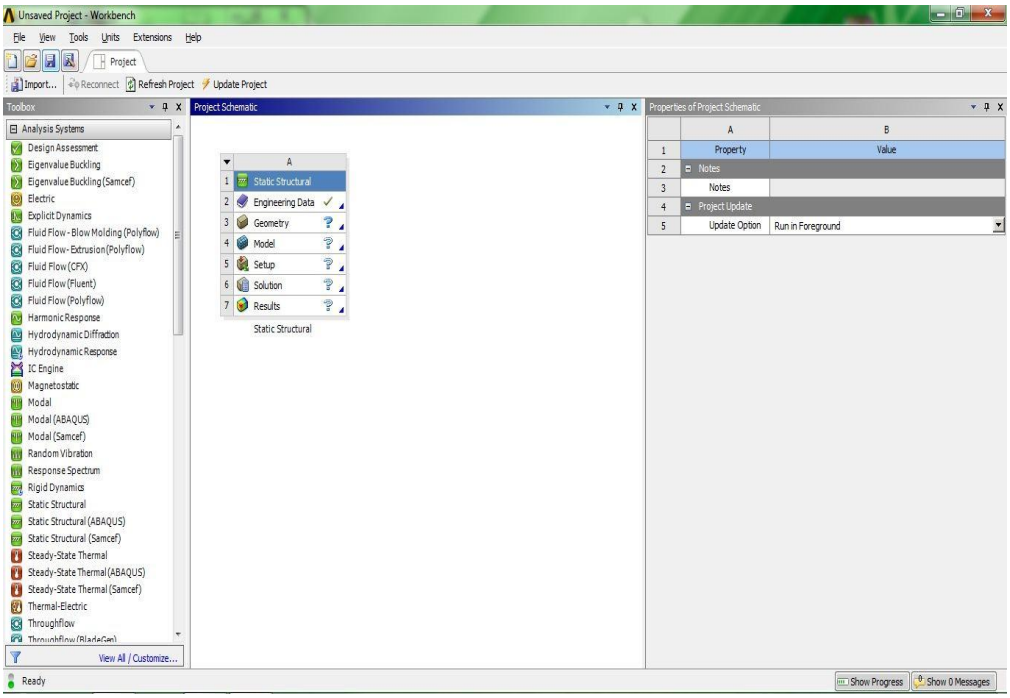

Figure 2.1: ANSYS (R17.0) Graphical User Interface (GUI).

➢ Preprocessor:

Within the preprocessor the model is set up. It usually includes a number of steps in the following order:

- **Build geometry**: Depending on whether the problem geometry is one, two or three dimensional, the geometry consists of creating lines, areas or volumes. These geometries can then, if necessary, be used to create other geometries by the use of Boolean operations. The key idea when building the geometry like this is to simplify the generation of the element mesh. Hence, this step is optional but most often used. Nodes and elements can however be created from coordinates only.

- **Define materials**: A material is defined by its material constants. Every element has to be assigned a particular material.

- **Generate element mesh**: The problem is treated by nodal points. The nodes are connected to form finite elements, which together form the material volume. Depending on the problem and the assumptions that are made, the element type has to be determined. Common element types are truss, beam, plate, shell and solid elements.

  The element mesh can in ANSYS be created in several ways. The most common way is that it is automatically created, however more or less controlled. For example, you can specify a certain number of elements in a specific area, or you can force the mesh generator to maintain a specific element size within an area. Certain element shapes or sizes are not recommended and if these limits are violated, a warning will be generated in ANSYS. It is up to the user to create a mesh which is able to generate results with a sufficient degree of accuracy.

➢ **Solution processor:**

Here we can solve the problem by gathering all specified information about the problem:

- **Apply loads**: Boundary conditions are usually applied on nodes or elements. The prescribed quantity can for example be force, traction, displacement, moment, rotation. The loads may also be edited from the preprocessor in ANSYS.

- **Obtain solution**: The solution to the problem can be obtained if the whole problem is defined.

➢ **Postprocessor:**

Within this part of the analysis we can for example:

- **Visualize the results**: like plot the deformed shape of the geometry or stresses.
- **List the results**: It is possible to list the results as tabular listings or file printouts.

2.5 Explicit Dynamics Analysis System *

2.5.1 Explicit Dynamics Applications

The Explicit Dynamics system is designed to simulate nonlinear structural mechanics applications involving one or more of the following:

- Impact from low [1m/s] to very high velocity [5000m/s].
- Stress wave propagation.
- High frequency dynamic response.
- Large deformations and geometric nonlinearities.
- Complex contact conditions.
- Complex material behavior including material damage and failure.
- Nonlinear structural response including buckling.
- Failure of bonds, welds, and fasteners.
- Shock wave propagation through solids and liquids.
- Rigid and flexible bodies.

Explicit Dynamics is most suited to events which take place over short periods of time, a few milliseconds or less. Events which last more than one second can be modeled; however, long run times can be expected. Techniques such as mass scaling and dynamic relaxation are available to improve the efficiency of simulations with long durations.

2.5.2 System Solving Strategy

In an Explicit Dynamics solution, we start with a discretized domain (meshing) with assigned material properties, loads, constraints and initial conditions. This initial state, when integrated in time, will produce motion at the node points in the mesh. The following steps explain the solution strategy in the explicit dynamics analysis system:

- The motion of the node points produces deformation in the elements of the mesh.
- The deformation results in a change in volume (hence density) of the material in each element.
- The rate of deformation is used to derive material strain rates using various element formulations.
- Constitutive laws take the material strain rates and derive resultant material stresses.

(*): All equations shown in this section are refer to reference [9].

- The material stresses are transformed back into nodal forces using various element formulations.
- External nodal forces are computed from boundary conditions, loads and contact (body interaction).
- The nodal forces are divided by nodal mass to produce nodal accelerations.
- The accelerations are integrated Explicitly in time to produce new nodal velocities.
- The nodal velocities are integrated Explicitly in time to produce new nodal positions.
- The solution process (Cycle) is repeated until a user defined time is reached. Figure (2.2) shows the solution process (cycle) algorithm.

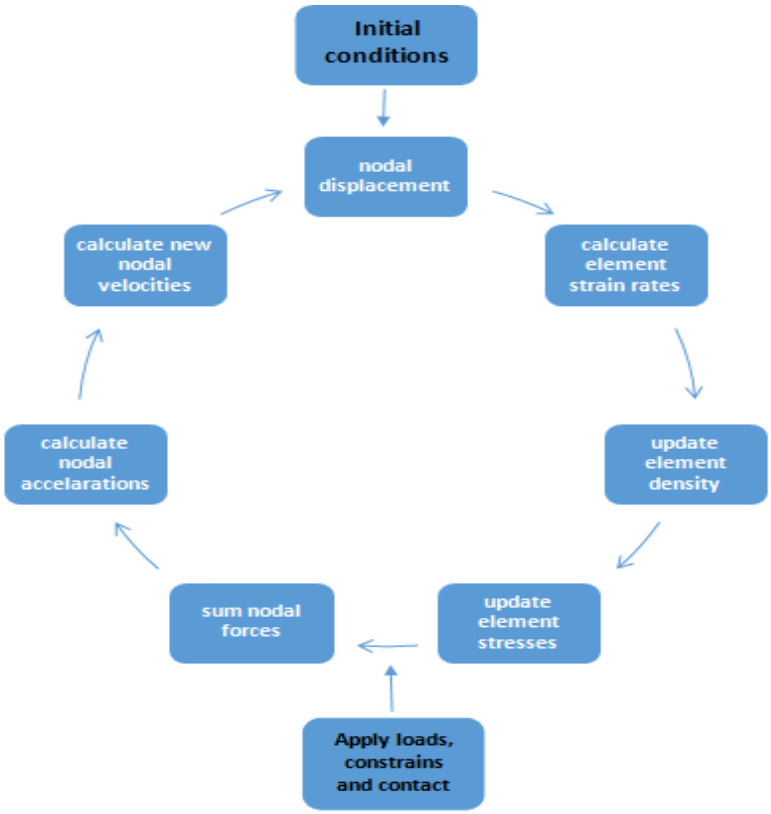

Figure 2.2: Explicit dynamics solution algorithm.

2.5.3 Explicit transient dynamics

The partial differential equations to be solved in an Explicit Dynamics analysis express the conservation of mass, momentum, and energy in Lagrangian coordinates. These, together with a material model and a set of initial and boundary conditions, define the complete solution of the problem.

For the Lagrangian formulations currently available in the Explicit Dynamics system, the mesh moves and distorts with the material it models and conservation of mass is automatically satisfied. The density at any time can be determined from the current volume of the zone and its initial mass, as:

$$\frac{\rho_0 V_0}{V} = \frac{m}{V} \tag{2-1}$$

The partial differential equations that express the conservation of momentum relate the acceleration to the stress tensor σ_{ij} , shown as:

$$\rho\ddot{x} = b_x + \frac{\partial \sigma_{xx}}{\partial x} + \frac{\partial \sigma_{xy}}{\partial y} + \frac{\partial \sigma_{xz}}{\partial z} \tag{2-2}$$

$$\rho\ddot{y} = b_y + \frac{\partial \sigma_{yx}}{\partial x} + \frac{\partial \sigma_{yy}}{\partial y} + \frac{\partial \sigma_{yz}}{\partial z} \tag{2-3}$$

$$\rho\ddot{z} = b_z + \frac{\partial \sigma_{zx}}{\partial x} + \frac{\partial \sigma_{zy}}{\partial y} + \frac{\partial \sigma_{zz}}{\partial z} \tag{2-4}$$

Conservation of energy is expressed via:

$$\dot{e} = \frac{1}{\rho}(\sigma_{xx}\dot{\varepsilon}_{xx} + \sigma_{yy}\dot{\varepsilon}_{yy} + \sigma_{zz}\dot{\varepsilon}_{zz} + 2\sigma_{xy}\dot{\varepsilon}_{xy} + 2\sigma_{yz}\dot{\varepsilon}_{yz} + 2\sigma_{zx}\dot{\varepsilon}_{zx}) \tag{2-5}$$

These equations are solved explicitly for each element in the model, based on input values at the end of the previous time step. Small time increments are used to ensure stability and accuracy of the solution. Note that in Explicit Dynamics we do not seek any form of equilibrium; we simply take results from the previous time point to predict results at the next time point. There is no requirement for iteration.

In a well-posed Explicit Dynamics simulation, mass, momentum, and energy should be conserved. Only mass and momentum conservation is enforced. Energy is accumulated over time and conservation is monitored during the solution. Feedback on the quality of the solution is provided via summaries of momentum and energy conservation (as opposed to convergent tolerances in implicit transient dynamics).

2.5.4 Explicit Time Integration

The Explicit Dynamic solver uses a central difference time integration scheme. After forces have been computed at the nodes of the mesh (resulting from internal stress, contact, or boundary conditions), the nodal accelerations are derived by equating acceleration to force divided by mass. Therefore, the accelerations are:

$$\ddot{x}_i = \frac{F_i}{m} + b_i \tag{2-6}$$

where:

$\ddot{x}_i$: are the components of nodal acceleration (i =1,2,3).

F_i : are the forces acting on the nodal points.

b_i : are the components of body acceleration.

m : is the mass attributed to the node.

With the accelerations at time (n) determined, the velocities at time (n+1/2) are found from:

$$\dot{x}_i^{n+1/2} = \dot{x}_i^{n-1/2} + \ddot{x}_i^n \Delta t^n \tag{2-7}$$

and finally, the positions are updated to time (n+1) by integrating the velocities as shown:

$$x_i^{n+1} = x_i^n + \dot{x}_i^{n+1/2} \Delta t^{n+1/2} \tag{2-8}$$

The advantages of using this method for time integration for nonlinear problems are:

- The equations become uncoupled and can be solved directly (explicitly). There is no requirement for iteration during time integration.
- No convergence checks are needed because the equations are uncoupled.
- No inversion of the stiffness matrix is required. All nonlinearities (including contact) are included in the internal force vector.

To ensure stability and accuracy of the solution, the size of the time step used in Explicit time integration is limited by the CFL (Courant-Friedrichs-Lewy) condition. This condition implies that the time step be limited such that a disturbance (stress wave) cannot travel farther than the smallest characteristic element dimension in the mesh, in a single time step. Thus the time step criteria for solution stability is:

$$\Delta t \leq f * \left[\frac{h}{c}\right]_{min} \tag{2-9}$$

where:

Δt : is the time increment.

f : is the stability time step factor.

h : is the characteristic dimension of an element.

c : is the local material sound speed in an element.

2.6 Verification of results

In recent years, the use of finite element analysis as a design tool has grown rapidly. Easy-to-use comprehensive packages such as ANSYS have become a common tool in the hands of design engineers. Unfortunately, many engineers without the proper training or a solid understanding of the underlying concepts have been using finite element analysis. Engineers who use finite element analysis must understand the limitations of the finite element procedures. There are various sources of error that can contribute to incorrect results. They include:

1. **Wrong input data**, such as physical properties and dimensions: This mistake can be corrected by simply listing and verifying physical properties and coordinates of nodes or key points before proceeding any further with the analysis.

2. **Selecting inappropriate types of elements**: Understanding the underlying theory will benefit in the most of this respects, needed to fully grasp the limitations of a given type of element and understand to which type of problems it applies.

3. **Poor element shape and size after meshing**: This area is a very important part of any finite element analysis. Inappropriate element shape and size will influence the accuracy of processing results. It is important that the user understands the difference between free meshing (using mixed-area element shapes) and mapped meshing (using all quadrilateral area elements or all hexahedral volume elements) and the limitations associated with them.

4. **Applying wrong boundary conditions and loads**: This step is usually the most difficult aspect of modeling. It involves taking an actual problem and estimating the loading and the appropriate boundary conditions for a finite element model. this step requires good judgment and some experience.

It is wise to spend some time to gain a full understanding of a problem before initiating a finite element model of the problem. There may even exist a reasonable solution form to the problem, and thus we can save a lots of time and effort.

2.7 Impulse Momentum and Impact *

2.7.1 Linear Impulse and Linear Momentum

2.7.1.1 For Particles

Consider the general curvilinear motion in space of a particle of mass *m*, figure (2.3), where the particle is located by its position vector *r* measured from a fixed origin *O*. The velocity of the particle is $v = \dot{r}$ and is tangent to its path (shown as a dashed line). The resultant *ΣF* of all forces on *m* is in the direction of its acceleration $\dot{v}$. We may now write the basic equation of motion for the particle, *ΣF* = *ma*, as:

$$\Sigma F = m\dot{v} = \frac{d}{dt}(mv) \qquad \textbf{or} \qquad \Sigma F = \dot{G} \tag{2-10}$$

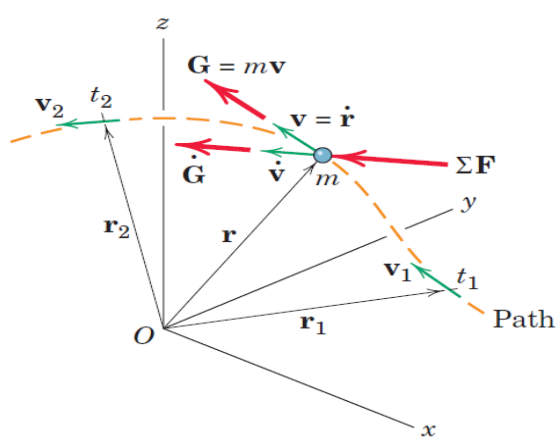

Figure 2.3: General curvilinear motion in space of a particle of mass *m*.

(*): All equations shown in this section are refer to reference [10].

Where the product of the mass and velocity is defined as the linear momentum $G = mv$ of the particle. Equation (2-10) states that the resultant of all forces acting on a particle equals its time rate of change of linear momentum. In *SI* the units of linear momentum mv are seen to be ($Kg.m/s$), which also equals ($N.s$).

Because Eq. (2-10) is a vector equation, we recognize that, in addition to the equality of the magnitudes of ΣF and $\dot{G}$, the direction of the resultant force coincides with the direction of the rate of change in linear momentum, which is the direction of the rate of change in velocity. Equation (2-10) is one of the most useful and important relationships in dynamics, and it is valid as long as the mass m of the particle is not changing with time. We now write the three scalar components of Eq. (2-10) as:

$$\Sigma F_x = \dot{G}_x \Sigma F_y = \dot{G}_y \Sigma F_z = \dot{G}_z \qquad (2\text{-}11)$$

where, these equations may be applied independently of one another.

All that we have done so far is to rewrite Newton's second law in an alternative form in terms of momentum. But we are now able to describe the effect of the resultant force ΣF on the linear momentum of the particle over a finite period of time simply by integrating Eq. (2-10) with respect to the time t. Multiplying the equation by dt gives $\Sigma F\ dt = dG$, which we integrate from time t_1 to time t_2 to obtain:

$$\int_{t1}^{t2} \Sigma F\ dt = G_2 - G_1 = \Delta G \qquad (2\text{-}12)$$

Here the linear momentum at time t_2 is $G_2 = mv_2$ and the linear momentum at time t_1 is $G_1 = mv_1$. The product of force and time is defined as the linear impulse of the force, and Eq. (2-12) states that the total linear impulse on m equals the corresponding change in linear momentum of m. Alternatively, we may write Eq. (2-12) as:

$$G_1 + \int_{t1}^{t2} \Sigma F\ dt = G_2 \qquad (2\text{-}12,a)$$

which says that the initial linear momentum of the body plus the linear impulse applied to it equals its final linear momentum.

The impulse integral is a vector which, in general, may involve changes in both magnitude and direction during the time interval. Under these conditions, it will be necessary to express ΣF and G in component form and then combine the integrated components. The components of Eq. (2-12,*a*) are the scalar equations:

$$m(v_1)_x + \int_{t1}^{t2} \Sigma F_x \, dt = m(v_2)_x$$

$$m(v_1)_y + \int_{t1}^{t2} \Sigma F_y \, dt = m(v_2)_y \qquad \text{(2-12,b)}$$

$$m(v_1)_z + \int_{t1}^{t2} \Sigma F_z \, dt = m(v_2)_z$$

These three scalar impulse-momentum equations are completely independent. Whereas Eq. (2-12) clearly stresses that the external linear impulse causes a change in the linear momentum, the order of the terms in Eqs. (2-12,*a*) and (2-12,*b*) corresponds to the natural sequence of events.

We now introduce the concept of the impulse-momentum diagram. Once the body to be analyzed has been clearly identified and isolated, we construct three drawings of the body as shown in figure (2.4). In the first drawing, we show the initial momentum *mv1*, or components thereof. In the second or middle drawing, we show all the external linear impulses (or components thereof). In the final drawing, we show the final linear momentum *mv2* (or its components). The writing of the impulse-momentum equations (2-12,*b*) then follows directly from these drawings, with a clear one-to-one correspondence between diagrams and equation terms.

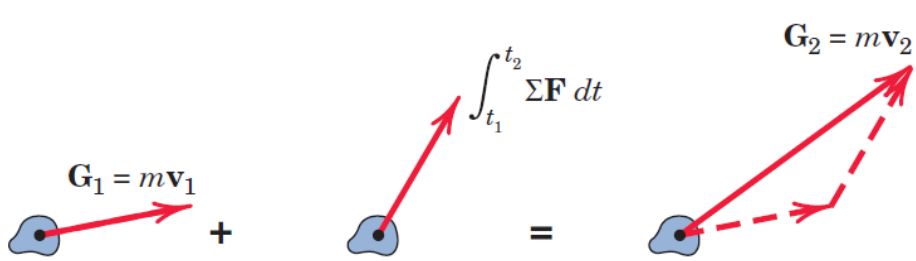

Figure 2.4: Impulse-Momentum diagram.

In some cases, certain forces are very large and of short duration. Such forces are called impulsive forces. An example is a force of sharp impact. There are cases where a force acting on a particle varies with the time in a manner determined by experimental measurements or by other

approximate means. In this case a graphical or numerical integration must be performed. If, for example, a force F acting on a particle in a given direction varies with the time t as indicated in figure (2.5) , then the impulse, $\int_{t1}^{t2} \Sigma F\, dt$, of this force from t_1 to t_2 is the shaded area under the curve.

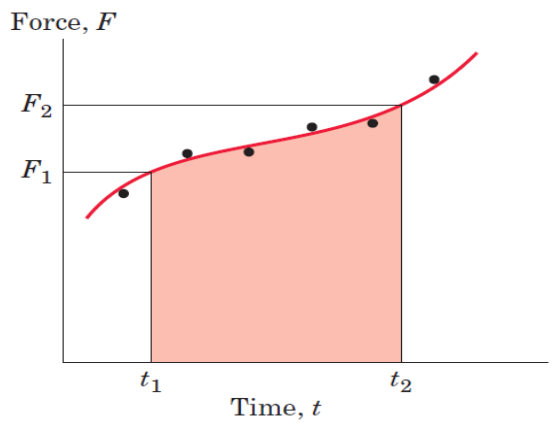

Figure 2.5: Force-Time diagram.

2.7.1.2 For System of Particles

From our definition in subsection (2.7.1.1), the linear momentum of the representative particle of the system depicted in figure (2.6) is $G_i = m_i v_i$ where the velocity of m_i is $v_i = \dot{r}_i$.The linear momentum of the system is defined as the vector sum of the linear momentum of all of its particles, or $G_i = \Sigma m_i v_i$. By substituting the relative-velocity relation, we obtain:

$$G = m\bar{v} \tag{2-13}$$

Thus, the linear momentum of any system of constant mass is the product of the mass and the velocity of its center of mass. The time derivative of G is $\dot{\bar{v}} = m\bar{a}$, which by equation($\Sigma F = m\ddot{\bar{r}} = m\bar{a}$) is the resultant external force acting on the system. Thus, we have:

$$\Sigma F = \dot{G} \tag{2-14}$$

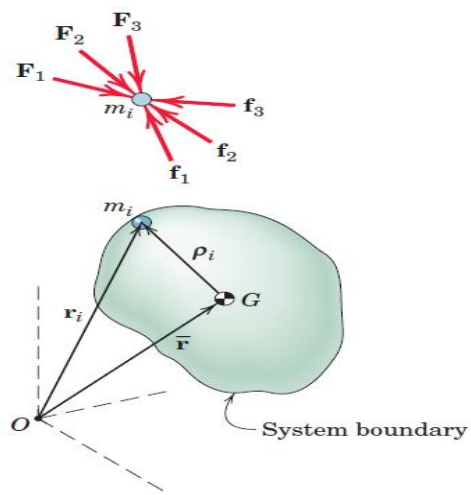

Figure 2.6: Representative particle of mass $\boldsymbol{m_i}$.

which has the same form as Eq. (2-10) for a single particle. Equation (2-14) states that the resultant of the external forces on any mass system equals the time rate of change of the linear momentum of the system. It is an alternative form of the generalized second law of motion,$\Sigma F = m\bar{a}$. As was noted, ΣF, in general, does not pass through the mass center G. In deriving Eq. (2-14), we differentiated with respect to time and assumed that the total mass is constant. Thus, the equation does not apply to systems whose mass changes with time.

2.7.1.3 For Rigid Bodies.

The principles of impulse and momentum were developed and used in subsection (2.7.1.1) for the description of particle motion. In that treatment, we observed that those principles were of particular importance when the applied forces were expressible as functions of the time and when interactions between particles occurred during short periods of time, such as with impact. Similar advantages result when the impulse momentum principles are applied to the motion of rigid bodies.

In subsection (2.7.1.2) the impulse-momentum principles were extended to cover any defined system of mass particles without restriction as to the connections between the particles of the system. These extended relations all apply to the motion of a rigid body, which is merely a special case of a general system of mass. We will now apply these equations directly to rigid-body motion.

We defined the linear momentum of a mass system as the vector sum of the linear momentum of all its particles and wrote $G_i = \Sigma m_i v_i$. With r_i representing the position vector to m_i, we have $v_i = \dot{r}_i$

and $G = \Sigma m_i \dot{r}_i$ which, for a system whose total mass is constant, may be written as $G = d(\Sigma m_i r_i)/dt$. When we substitute the principle of moments $m\bar{r} = \Sigma m_i r_i$ to locate the mass center, the momentum becomes $G = d(m\bar{r})/dt = m\dot{\bar{r}}$, where $\dot{\bar{r}}$ is the velocity $\bar{v}$ of the mass center. Therefore, as before, we find that the linear momentum of any mass system, rigid or non-rigid, is:

$$G = m\bar{v} \tag{2-15}$$

We rewrote Newton's generalized second law as Eq. (2-14). This equation and its integrated form are:

$$\Sigma F = \dot{G} \qquad \text{and} \qquad G_1 + \int_{t1}^{t2} \Sigma F \, dt = G_2 \tag{2-16}$$

Equation (2-16) may be written in its scalar component form as:

$$\Sigma F_x = \dot{G}_x \qquad (G_x)_1 + \int_{t1}^{t2} \Sigma F_x \, dt = (G_x)_2$$

$$\Sigma F_y = \dot{G}_y \qquad \text{and} \qquad (G_y)_1 + \int_{t1}^{t2} \Sigma F_y \, dt = (G_y)_2 \tag{2-16,a}$$

$$\Sigma F_z = \dot{G}_z \qquad (G_z)_1 + \int_{t1}^{t2} \Sigma F_z \, dt = (G_z)_2$$

In words, the first of Eqs. (2-16) and (2-16,*a*) states that the resultant force equals the time rate of change of momentum. The integrated form of Eqs. (2-16) and (2-16,*a*) states that the initial linear momentum plus the linear impulse acting on the body equals the final linear momentum.

As in the force-mass-acceleration formulation, the force summations in Eqs. (2-16) and (2-16,*a*) must include all forces acting externally on the body considered. We emphasize again, therefore, that in the use of the impulse-momentum equations, it is essential to construct the complete impulse-momentum diagrams so as to disclose all external impulses. In contrast to the method of work and energy, all forces exert impulses, whether they do work or not.

2.7.2 Impacts of Particles

The principles of impulse and momentum have important use in describing the behavior of colliding bodies. Impact refers to the collision between two bodies and is characterized by the generation of relatively large contact forces which act over a very short interval of time. It is important to realize that an impact is a very complex event involving material deformation and recovery and the generation of heat and sound. Small changes in the impact conditions may cause large changes in the impact process and thus in the conditions immediately following the impact.

2.7.2.1 Direct Central Impact

As an introduction to impact, we consider the collinear motion of two spheres of masses m_1 and m_2 , figure (2.7), traveling with velocities v_1 and v_2. If v_1 is greater than v_2, collision occurs with the contact forces directed along the line of centers. This condition is called direct central impact.

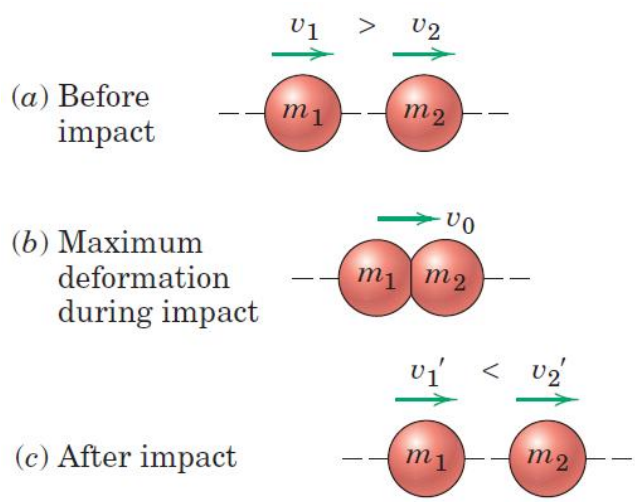

Figure 2.7: Collinear motion and impacts of two spheres.

Following initial contact, a short period of increasing deformation takes place until the contact area between the spheres ceases to increase. At this instant, both spheres, figure (2.7*b*), are moving with the same velocity v_0. During the remainder of contact, a period of restoration occurs during which the contact area decreases to zero. In the final condition shown in part (*c*) of the figure, the spheres now have new velocities v_1' and v_2' where v_1' must be less than v_2'. All velocities are arbitrarily

assumed positive to the right, so that with this scalar notation a velocity to the left would carry a negative sign. If the impact is not overly severe and if the spheres are highly elastic, they will regain their original shape following the restoration. With a more severe impact and with less elastic bodies, a permanent deformation may result.

Because the contact forces are equal and opposite during impact, the linear momentum of the system remains unchanged, as discussed in subsection (2.7.1.1). Thus, we apply the law of conservation of linear momentum and write as:

$$m_1 v_1 + m_2 v_2 = m_1 \grave{v}_1 + m_2 \grave{v}_2 \tag{2-17}$$

We assume that any forces acting on the spheres during impact, other than the large internal forces of contact, are relatively small and produce negligible impulses compared with the impulse associated with each internal impact force. In addition, we assume that no appreciable change in the positions of the mass centers occurs during the short duration of the impact.

2.7.2.2 Coefficient of Restitution

For given masses and initial conditions, the momentum equation contains two unknowns, $\grave{v}_1$ and $\grave{v}_2$ clearly, we need an additional relationship to find the final velocities. This relationship must reflect the capacity of the contacting bodies to recover from the impact and can be expressed by the ratio (e) of the magnitude of the restoration impulse to the magnitude of the deformation impulse. This ratio is called the coefficient of restitution.

Let F_r and F_d represent the magnitudes of the contact forces during the restoration and deformation periods, respectively, as shown in figure (2.9). For particles, the definition of e together with the impulse momentum equation given as:

$$e = \frac{\int_{t_0}^{t} F_r \, dt}{\int_0^{t_0} F_d \, dt} = \frac{\grave{v}_2 - \grave{v}_1}{v_1 - v_2} = \frac{|relative \;\; velocity \;\; of \;\; separation \;\; |}{|relative \;\; velocity \;\; of \;\; approac \;\; h|} \tag{2-18}$$

We are careful in these equations to express the change of momentum (and therefore Δv) in the same direction as the impulse (and thus the force). The time for the deformation is taken as t_0 and the total time of contact is t. If the two initial velocities v_1 and v_2 and the coefficient of restitution e are known, then Eqs. (2-17) and (2-18) give us two equations in the two unknown final velocities $\grave{v}_1$ and $\grave{v}_2$.

2.7.3 Impacts of Rigid Bodies

Impact phenomena involve a fairly complex interrelationship of energy and momentum transfer, energy dissipation, elastic and plastic deformation, relative impact velocity, and body geometry. In section (2.7.2) we treated the impact of bodies modeled as particles and considered only the case of central impact, where the contact forces of impact passed through the mass centers of the bodies, as would always happen with colliding smooth spheres, for example. To relate the conditions after impact to those before impact required the introduction of the so-called coefficient of restitution e or impact coefficient, which compares the relative separation velocity with the relative approach velocity measured along the direction of the contact forces. Although in the classical theory of impact, e was considered a constant for given materials, more modern investigations show that e is highly dependent on geometry and impact velocity as well as on materials. At best, even for spheres and rods under direct central and longitudinal impact, the coefficient of restitution is a complex and variable factor of limited use.

Any attempt to extend this simplified theory of impact utilizing a coefficient of restitution for the non-central impact of rigid bodies of varying shape is a gross oversimplification which has little practical value.

2.8 Stress and Strain Analysis *

2.8.1 Stress and Strain Definitions

The most fundamental concepts in the strength of materials science are stress and strain. These concepts can be illustrated in their most elementary form by considering a prismatic bar subjected

(*): All equations shown in this section are refer to reference [11].

to axial forces. A prismatic bar is a straight structural member having the same cross section throughout its length, and an axial force is a load directed along the axis of the member, resulting in either tension or compression in the bar. Where figure (2.8) describe the prismatic bar in tension condition. The prismatic bar examples appear clearly in the members of a bridge truss, connecting rods in automobile engines, spokes of bicycle wheels, columns in buildings, and wing struts in small airplanes.

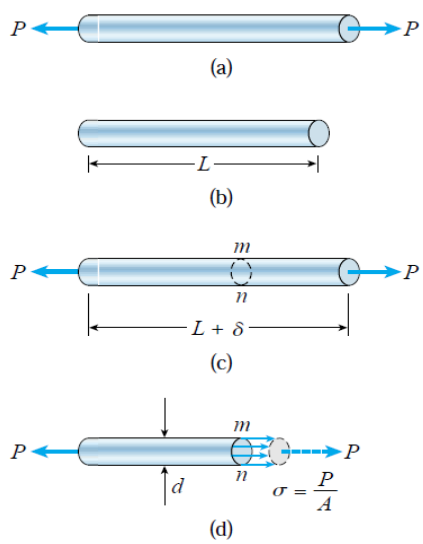

Figure 2.8: Prismatic bar in tension: (a) free-body diagram of a segment of the bar, (b) segment of the bar before loading, (c) segment of the bar after loading, and (d) normal stresses in the bar

When drawing the free-body diagram (Fig. 2.8,*a*), we disregard the weight of the bar itself and assume that the only active forces are the axial forces P at the ends. Next we consider two views of the bar, the first showing the same bar before the loads are applied (Fig. 2.8,*b*) and the second showing it after the loads are applied (Fig. 2.8,*c*). Note that the original length of the bar is denoted by the letter L, and the increase in length due to the loads is denoted by the Greek letter δ (delta).

The internal actions in the bar are exposed if we make an imaginary cut through the bar at section *m-n* (Fig. 2.8,*c*). Because this section is taken perpendicular to the longitudinal axis of the bar, it is called a cross section. We now isolate the part of the bar to the left of cross section *m-n* as a free body (Fig. 2.8,*d*). At the right-hand end of this free body (section *m-n*) we show the action of the removed part of the bar (that is, the part to the right of section *m-n*) upon the part that remains. This action consists of continuously distributed stresses acting over the entire cross section, and the axial force P acting at the cross section is the resultant of those stresses (The resultant force is shown with a dashed line in Fig. (2.8,*d*)). Stress has units of force per unit area and is denoted by the Greek letter σ (sigma).

In general, the stresses acting on a plane surface may be uniform throughout the area or may vary in intensity from one point to another. Let us assume that the stresses acting on cross section *m-n* (Fig.2.8,*d*) are uniformly distributed over the area. Then the resultant of those stresses must be equal to the magnitude of the stress times the cross-sectional area *A* of the bar, that is, $P = \sigma * A$. Therefore, we obtain the following expression for the magnitude of the stresses:

$$\sigma = \frac{P}{A} \tag{2.19}$$

This equation gives the intensity of uniform stress in an axially loaded, prismatic bar of arbitrary cross-sectional shape, which valid only if the stress is uniformly distributed over the cross section of the bar. This condition is realized if the axial force *P* acts through the centroid of the cross-sectional area. But, when the load *P* does not act at the centroid, bending of the bar will result and a more complicated analysis is necessary, where this equation is still be useful because it gives the average normal stress on the cross section.

The uniform stress condition pictured in figure (2.8,d) exists throughout the length of the bar except near the ends. The stress distribution at the end of a bar depends upon how the load P is transmitted to the bar. If the load happens to be distributed uniformly over the end, then the stress pattern at the end will be the same as everywhere else. However, it is more likely that the load is transmitted through a pin or a bolt, producing high localized stresses called stress concentrations.

When the bar is stretched by the forces *P*, the stresses are tensile stresses; if the forces are reversed in direction, causing the bar to be compressed, we obtain compressive stresses. Inasmuch as the stresses act in a direction perpendicular to the cut surface, they are called normal stresses. Thus, normal stresses may be either tensile or compressive. If the stresses act in a direction tangential to the cut surface, they are called shear stress, which customarily denoted by the Greek letter τ (tau). When a sign convention for normal stresses is required, it is customary to define tensile stresses as positive and compressive stresses as negative. Because the normal stress (σ) is obtained by dividing the axial force by the cross-sectional area, it has units of force per unit of area. When *SI* units are used, force is expressed in Newton (*N*) and area in square meters (m^2). Consequently, stress has units of Newton per square meter (N/m^2), that is, Pascal's (*Pa*).

As already observed, a straight bar will change in length when loaded axially, becoming longer when in tension and shorter when in compression. For instance, consider again the prismatic bar of figure (2.8). The elongation δ of this bar (Fig. 2.8,*c*) is the cumulative result of the stretching of all elements of the material throughout the volume of the bar. Let us assume that the material is the

same everywhere in the bar. Then, if we consider half of the bar (length $L/2$), it will have an elongation equal to ($\delta/2$), and so on.

In general, the elongation of a segment is equal to its length divided by the total length L and multiplied by the total elongation δ. Therefore, a unit length of the bar will have an elongation equal to $1/L$ times δ. This quantity is called the elongation per unit length, or strain, and is denoted by the Greek letter ε (epsilon). We see that strain is given by the equation:

$$\varepsilon = \frac{\delta}{L} \tag{2.20}$$

If the bar is in tension, the strain is called a tensile strain, representing an elongation or stretching of the material. If the bar is in compression, the strain is a compressive strain and the bar shortens. Tensile strain is usually taken as positive, and compressive strain as negative. The strain (ε) is called a normal strain because it is associated with normal stresses. Because normal strain is the ratio of two lengths, it is a dimensionless quantity, that is, it has no units. Therefore, strain is expressed simply as a number, independent of any system of units. When the strain is associated with shear stress, an angled distortion will be formed. This angle is denoted by the Greek letter γ (gamma), and it will be called shear strain. Due to that shear strain is an angle, it is usually measured in degrees or radians.

2.8.2 Stress-Strain Diagram

The axial stress (σ) in a specimen, that affected by tensile stresses, is calculated by dividing the axial load P by the cross-sectional area A (Eq. 2.19). When the initial area of the specimen is used in the calculation, the stress is called the nominal stress (other names are conventional stress and engineering stress). A more exact value of the axial stress, called the true stress, can be calculated by using the actual area of the bar at the cross section where failure occurs, when the specimen is fracture. Since the actual area in a tension effect is always less than the initial area, the true stress is larger than the nominal stress.

Also, the average axial strain (ε) in the specimen is found by dividing the measured elongation (δ) between the gage marks by the specimen length L. If the initial length is used in the calculation, the nominal strain is obtained. Since the distance between the gage marks increases as the tensile load

is applied, we can calculate the true strain (or natural strain) at any value of the load by using the actual specimen length. As the actual length is larger than the initial length, the true strain is always smaller than nominal strain. However, for most engineering purposes, the nominal stress and nominal strain are adequate designing values.

After performing a tension or compression loading effect and determining the stress and strain values at various magnitude of the loads, we can plot a diagram of stress versus strain. Such as a stress-strain diagram, which is a characteristic of the particular material, that being loaded, and conveys important information about the mechanical properties and type of behavior.

The material that will be discuss is a structural steel, also known as mild steel or low-carbon steel. Structural steel is one of the most widely used metals and is found in buildings, bridges, cranes, ships, towers, vehicles, and many other types of construction. A stress-strain diagram for a typical structural steel in tension is shown in figure (2.9). Strains are plotted on the horizontal axis and stresses on the vertical axis. In order to display all of the important features of this material, the axis in the figure are not drawn to scale.

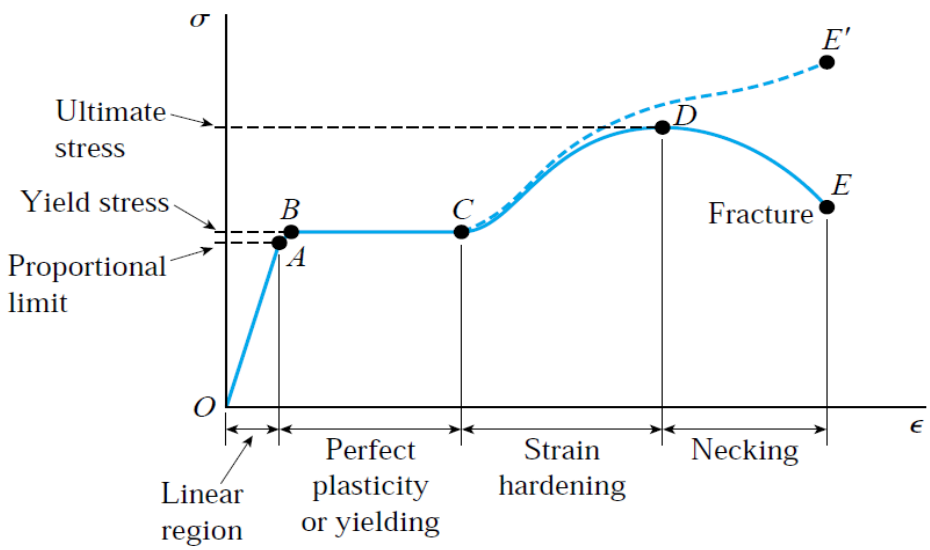

Figure 2.9: Stress-strain diagram for a typical structural steel in tension.

The diagram begins with a straight line from the origin *O* to point *A*, which means that the relationship between stress and strain in this initial region is not only linear but also proportional, their ratio's remains constant. Beyond point *A*, the proportionality between stress and strain no longer exists; hence the stress at *A* is called the proportional limit. For low-carbon steels, this limit

is in the range (210) to (350) *MPa*, but high-strength steels (with higher carbon content plus other alloys) can have proportional limits of more than (550) *MPa*. The slope of the straight line from *O* to *A* is called the modulus of elasticity. Because the slope has units of stress divided by strain, modulus of elasticity has the same units as stress.

With an increase in stress beyond the proportional limit, the strain begins to increase more rapidly for each increment in stress. Consequently, the stress-strain curve has a smaller and smaller slope, until, at point *B*, the curve becomes horizontal. Beginning at this point, considerable elongation of the test specimen occurs with no noticeable increase in the tensile force (from *B* to *C*). This phenomenon is known as yielding of the material, and point *B* is called the yield point. The corresponding stress is known as the yield stress of the steel.

In the region from *B* to *C*, the material becomes perfectly plastic, which means that it deforms without an increase in the applied load. After undergoing the large strains that occur during yielding in the region *BC*, the steel begins to strain harden. During strain hardening, the material undergoes changes in its crystalline structure, resulting in increased resistance of the material to further deformation. Elongation of the test specimen in this region requires an increase in the tensile load, and therefore the stress-strain diagram has a positive slope from *C* to *D*. The load eventually reaches its maximum value, and the corresponding stress (at point *D*) is called the ultimate stress. Further stretching of the bar is actually accompanied by a reduction in the load, and fracture finally occurs at a point such as *E* for engineering stress-strain curve, or *E'* for true stress-strain curve.

The yield stress and ultimate stress of a material are also called the yield strength and ultimate strength, respectively. Strength is a general term that refers to the capacity of a structure to resist loads. For instance, the yield strength of a beam is the magnitude of the load required to cause yielding in the beam, and the ultimate strength of a truss is the maximum load it can support, which is the failure load.

2.8.3 Elasticity and Plasticity Behavior of Materials

Stress-strain diagrams describe the behavior of engineering materials when the materials are loaded in tension or compression, as described in the preceding sub-section. To go one step further, consider what happens when the load is removed and the material is unloaded. Assume, for instance, that we apply a load to a tensile specimen so that the stress and strain go from the origin *O* to point *A* on the stress-strain curve of Figure (2.10,*a*). Suppose further that when the load is

removed, the material follows exactly the same curve back to the origin *O*. This property of a material, by which it returns to its original dimensions during unloading, is called elasticity, and the material itself is said to be elastic. Note that the stress-strain curve from *O* to *A* needn't be linear in order for the material to be elastic.

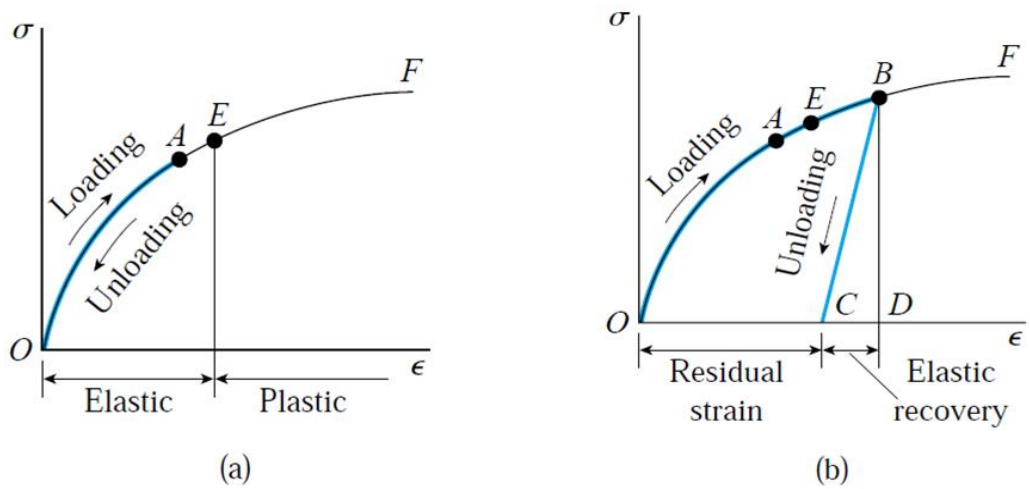

Figure 2.10: Stress-Strain diagrams illustrating (a) elastic behavior, and (b) partially elastic behavior.

Now suppose that the load affected same material to a higher level, so that point *B* is reached on the stress-strain curve (Fig. 2.10,*b*). When unloading occurs from point *B*, the material follows line *BC* on the diagram. This unloading line is parallel to the initial portion of the loading curve; that is, line *BC* is parallel to a tangent to the stress-strain curve at the origin. When point *C* is reached, the load has been entirely removed, but a residual strain, or permanent strain, represented by line *OC*, remains in the material. As a consequence, the bar being tested is longer than it was before loading. This residual elongation of the bar is called the permanent set. For the total strain *OD* developed during loading from *O* to *B*, the strain *CD* has been recovered elastically and the strain *OC* remains as a permanent strain. Thus, during unloading the bar returns partially to its original shape, and so the material is said to be partially elastic.

Between points *A* and *B* on the stress-strain curve (Fig. 2.10,*b*), there must be a point before which the material is elastic and beyond which the material is partially elastic. To find this point, we load the material to some selected value of stress and then remove the load. If there is no permanent set, that the value of elongation of the bar returns to zero, then the material is fully elastic up to the selected value of the stress. By this procedure, it is possible to determine the stress at the upper limit of the elastic region. For instance, the stress at point *E* in Figure (2.10) is the stress was known as the elastic limit of the material.

The characteristic of a material by which it undergoes inelastic strains beyond the strain at the elastic limit is known as plasticity. Thus, on the stress-strain curve of figure (2.10,*a*), their an elastic region followed by a plastic region. When large deformations occur in a ductile material loaded into the plastic region, the material is said to undergo plastic flow.

2.8.4 Hooke's Law and Poisson's Ratio Definitions

When a material behaves elastically and also exhibits a linear relationship between stress and strain, it is said to be linearly elastic. This type of behavior is extremely important in engineering design for an obvious reason, to design the structures and machines to function in this region and avoiding permanent deformations due to yielding.

The linear relationship between stress and strain for a bar in simple tension or compression is expressed by the equation:

$$\sigma = E\varepsilon \tag{2.21}$$

in which σ is the axial stress, ε is the axial strain, and E is a constant of proportionality known as the modulus of elasticity for the material, which also called the Young's modulus of material. The modulus of elasticity is the slope of the stress-strain diagram in the linearly elastic region. Since strain is dimensionless, the units of E are the same as the units of stress. Typical units of E are Pascal's in *SI* units.

Also, the proportional relationship between the shear stress and shear strain, in linearly elastic region, can be expressed by the equation:

$$\tau = G\gamma \tag{2.22}$$

in which τ is the shear stress, γ is the shear strain, and G is the shear modulus of elasticity, which also called the modulus of rigidity.

Equation (2.21) is commonly known as Hooke's law, named for the famous English scientist Robert Hooke (1635–1703), where equation (2.22) is known as Hooke's law in shear. Hooke was the first person to investigate scientifically the elastic properties of materials, and he tested such diverse materials as metal, wood, stone, and bone. He measured the stretching of long wires and observed their elongations. Thus, Hooke established the linear relationship between the applied loads and the resulting elongations.

Equation (2.21) is actually a very limited version of Hooke's law because it relates only to the longitudinal stresses and strains developed in simple tension or compression of a bar (uniaxial stress), which the same in Eq. (2.22). To deal with more complicated states of stress, such as those found in most structures and machines, more extensive equations of Hooke's law are needed.

When a prismatic bar is loaded in tension, the axial elongation is accompanied by lateral contraction, where the contraction is normal to the direction of the applied load. This change in shape is shown in figure (2.11), where part (*a*) shows the bar before loading and part (*b*) shows it after loading. In part (*b*), the dashed lines represent the shape of the bar before loading.

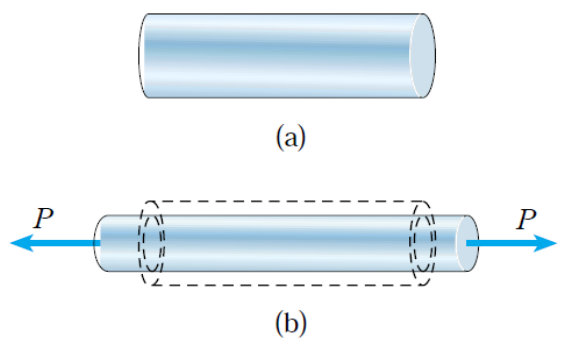

Figure 2.11: Axial elongation and lateral contraction of a prismatic bar in tension: (a) bar before loading, and (b) bar after loading.

Lateral contraction is easily seen by stretching a rubber band, but in metals the changes in lateral dimensions (in the linearly elastic region) are usually too small to be visible. However, they can be detected with sensitive measuring devices.

The lateral strain (ε') at any point in a bar is proportional to the axial strain (ε) at that same point if the material is linearly elastic. The ratio of these strains is a property of the material known as

Poisson's ratio. This dimensionless ratio, usually denoted by the Greek letter ν (nu), can be expressed by the equation:

$$\nu = -\frac{lat\,eral\ \ strain}{axial\ \ strain} = -\frac{\varepsilon'}{\varepsilon} \tag{2.23}$$

The minus sign is inserted in the equation to compensate for the fact that the lateral and axial strains normally have opposite signs. For instance, the axial strain in a bar in tension is positive and the lateral strain is negative, due to the decreasing in bar width. For compression we have the opposite situation, with the bar becoming shorter (negative axial strain) and wider (positive lateral strain). Therefore, for ordinary materials Poisson's ratio will have a positive value.

When Poisson's ratio for a material is known, we can obtain the lateral strain from the axial strain as follows:

$$\varepsilon' = -\nu\varepsilon \tag{2.24}$$

where these equations, (2.23) and (2.24), are applying only to a bar in uniaxial stress, that is, a bar for which the only stress is the normal stress (σ) in the axial direction.

When the strains in a material become large, Poisson's ratio changes. For example, in the case of structural steel the Poisson's ratio becomes larger in plastic yielding region comparing to the elastic region, which remains constant only in the linearly elastic range. When the material behavior is nonlinear, the ratio of lateral strain to axial strain is often called the contraction ratio. Of course, in the special case of linearly elastic behavior, the contraction ratio is the same as Poisson's ratio.

For a particular material, Poisson's ratio remains constant throughout the linearly elastic range, as explained previously. Therefore, at any given point in the prismatic bar of figure (2.11), the lateral strain remains proportional to the axial strain as the load increases or decreases. However, for a given value of the load, which means that the axial strain is constant throughout the bar, additional conditions must be met, if the lateral strains are to be the same throughout the entire bar.

Firstly, the material must be homogeneous, that is, it must have the same composition (and hence the same elastic properties) at every point. However, having a homogeneous material does not mean that the elastic properties at a particular point are the same in all directions. For instance, the

modulus of elasticity could be different in the axial and lateral directions. Therefore, a second condition for uniformity in the lateral strains is that the elastic properties must be the same in all directions perpendicular to the longitudinal axis. When the previous conditions are met, as is often the case with metals, the lateral strains in a prismatic bar subjected to uniform tension will be the same at every point in the bar and the same in all lateral directions.

Materials having the same properties in all directions, whether axial, lateral, or any other direction, are said to be isotropic. If the properties differ in various directions, the material is anisotropic.

2.8.5 Strain Energy Principle

The strain energy principles are widely used for determining the response of machines and structures to both static and dynamic loads. In this section introduce the subject of strain energy in its simplest form by considering only axially loaded members subjected to static loads.

To illustrate the basic ideas, consider a prismatic bar of length L subjected to a tensile force P, as shown in figure (2.12). And assuming that the load is applied slowly, so that it gradually increases from zero to its maximum value P. Such a load is called a static load because there are no dynamic or inertial effects due to motion. The bar gradually elongates as the load is applied, eventually reaching its maximum elongation (δ) at the same time that the load reaches its full value P. Thereafter, the load and elongation remain unchanged.

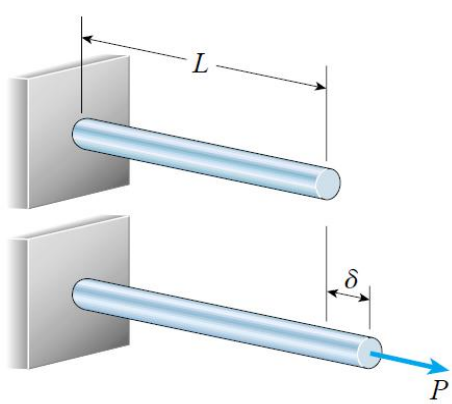

Figure 2.12: Prismatic bar subjected to a statically applied load.

During the loading process, the load P moves slowly through the distance δ and does a certain amount of work. To evaluate this work, recalling that a constant force does work equal to the product of the force and the distance through which it moves. However, in our case the force varies in magnitude from zero to its maximum value P. To find the work done by the load under these conditions, we need to know the behavior in which the force varies. This information is supplied by a load-displacement diagram, such as the one plotted in Fig. (2.13). On this diagram the vertical axis represents the axial load and the horizontal axis represents the corresponding elongation of the bar. The shape of the curve depends upon the properties of the material.

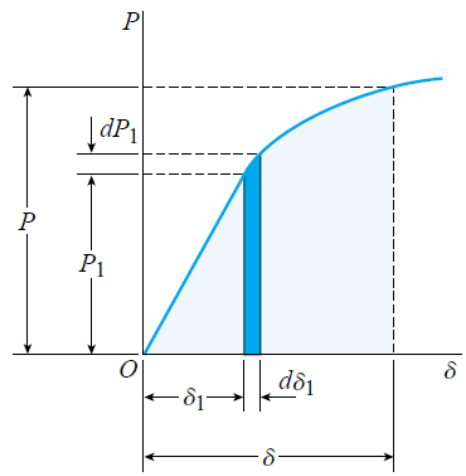

Figure 2.13: Load-displacement diagram.

Now, denote by P_1 any value of the load between zero and the maximum value P, and the corresponding elongation of the bar by δ_1. Then an increment dP_1 in the load will produce an increment $d\delta_1$ in the elongation. The work done by the load during this incremental elongation is the product of the load and the distance through which it moves, that is, the work equals $P_1 d\delta_1$. This work is represented in the figure by the area of the shaded strip below the load-displacement curve. The total work done by the load as it increases from zero to the maximum value P is the summation of all such elemental strips:

$$W = \int_0^{\delta} P_1 d\delta_1 \tag{2.25}$$

In geometric terms, the work done by the load is equal to the area below the load-displacement curve. Work are expressed in *SI* units by joule's (*J*), which is equal to one newton meter (1*J*=1*N.m*).

When the load stretches the bar, strains are produced. The presence of these strains increases the energy level of the bar itself. Therefore, a new quantity, called strain energy, is defined as the energy absorbed by the bar during the loading process. From the principle of conservation of energy, we know that this strain energy is equal to the work done by the load provided no energy is added or subtracted in the form of heat. Therefore,

$$U = W = \int_0^{\delta} P_1 d\delta_1 \tag{2.26}$$

in which U is the symbol for strain energy. Sometimes strain energy is referred to as internal work to distinguish it from the external work done by the load. Work and energy are expressed in the same units.

If the force P (Fig. 2.12) is slowly removed from the bar, the bar will shorten. If the elastic limit of the material is not exceeded, the bar will return to its original length. If the limit is exceeded, a permanent set will remain (Section 2.8.3). Thus, either all or part of the strain energy will be recovered in the form of work. This behavior is shown on the load-displacement diagram of Fig. (2.14). During loading, the work done by the load is equal to the area below the curve (area *OABCDO*). When the load is removed, the load-displacement diagram follows line *BD* if point *B* is beyond the elastic limit, and a permanent elongation *OD* remains. Thus, the strain energy recovered during unloading, called the elastic strain energy, is represented by the shaded triangle *BCD*. Area *OABDO* represents energy that is lost in the process of permanently deforming the bar. This energy is known as the inelastic strain energy.

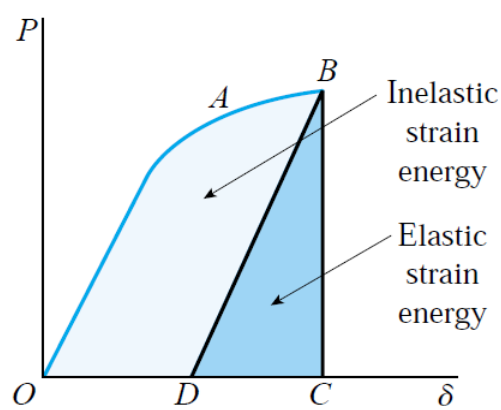

Figure 2.14: Elastic and inelastic strain energy.

Most structures are designed with the expectation that the material will remain within the elastic range under ordinary conditions of service. Assuming that the load at which the stress in the material reaches the elastic limit is represented by point *A* on the load-displacement curve (Fig.2.14). As long as the load is below this value, all of the strain energy is recovered during unloading and no permanent elongation remains. Thus, the bar acts as an elastic spring, storing and releasing energy as the load is applied and removed.

3

Chapter Three

Project Modeling Design and Results Clarification

3.1 Introduction.

3.2 Design Description.

3.2.1 Design Overview.

3.2.2 Models Description.

3.3 Simulation Methodology.

3.4 Results Clarification.

3.4.1 Simulation Results.

3.4.2 Results Discussion.

3.1 Introduction

The aim of this project is to study the impact of collision on the chassis of the vehicle. In this context, we have chosen a Land Rover Defender to subjected its basic structure (Defender's chassis) into collision analysis tests, where figure (3.1) shows a real basic chassis design for the Defender. The chassis structure models were drawn by using the CATIA program, and simulating their collision tests into ANSYS program.

Figure 3.1: Defender's chassis.

3.2 Design Description

3.2.1 Design Overview

Figure (3.1) shows the chassis of the Land Rover Defender, which is the main structure for all the Defender models since the start of manufacturing in 1983. The general development of the Defender until these days are the one of the simplest vehicle evolutions in the automotive industry, where the Defender is maintained its traditional shape design, and reflected this simplicity to its chassis design. The chassis evolution does not exceed the addition of some bridges with different cross sections.

The structure of the chassis consists of two longitudinal main bridges, carriers, extending along the chassis, were they connected to each other by a series of cross-bridges with different cross sections

and multi-positions located on these carriers. The carriers end up associating with the rear bumper, which is also a part in the chassis structure and serves as a cross-bridge. The chassis is made from structural steel material with square cross section and (4 mm) steel thickness in all the structure sections.

In this research, three models of the same vehicle chassis have been subjected to the collision analysis tests to compare their test results to each other. The first model, which the authors named "A-model", is the basic model of the Defender, without any significant additions of the middle cross-bridges, which shown in figures (3.1) and (3.2). The second model "B-model" is a model developed from the basic one by adding a cross-bridge in the front half of the chassis, which works as a gearbox carrier as shown in figure (3.3). The third and last model "C-model" is the latest development model for the Defender, which contains a middle cross-bridge, in the chassis structure, in addition to the previous "B-model", figure (3.4) shows the third model "C-model" with all addition bridges on it.

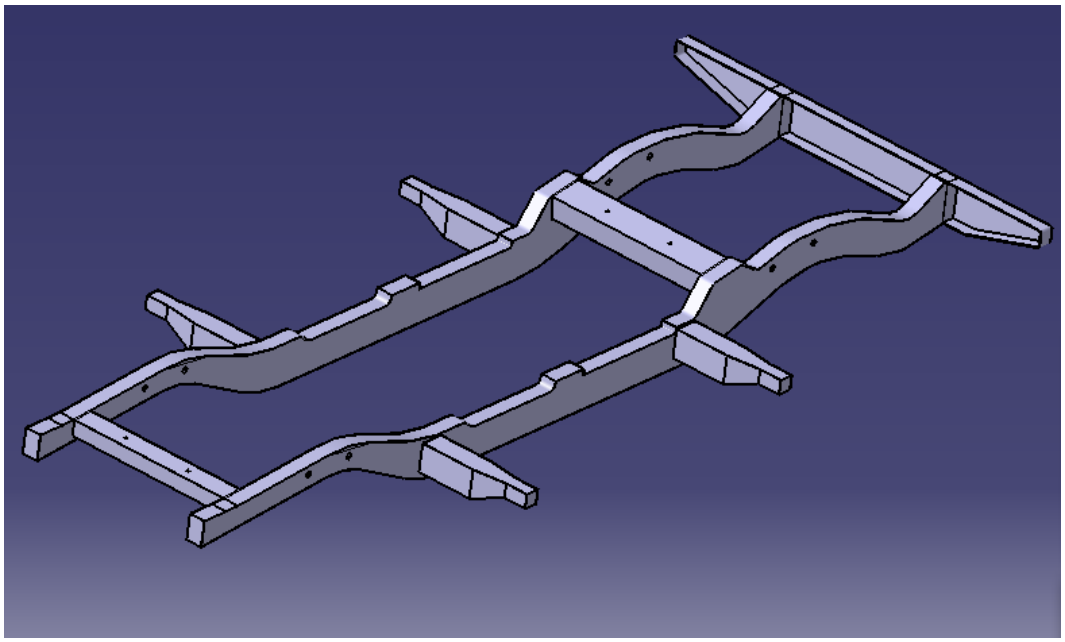

Figure 3.2: "A-model" design.

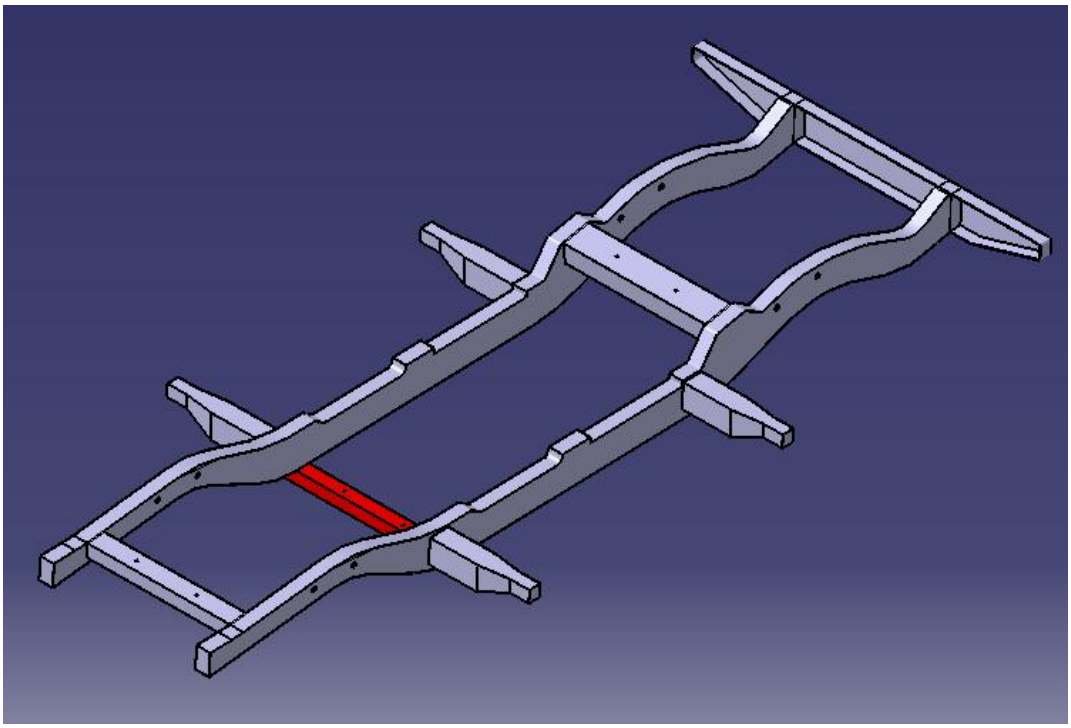

Figure 3.3: "B-model" design.

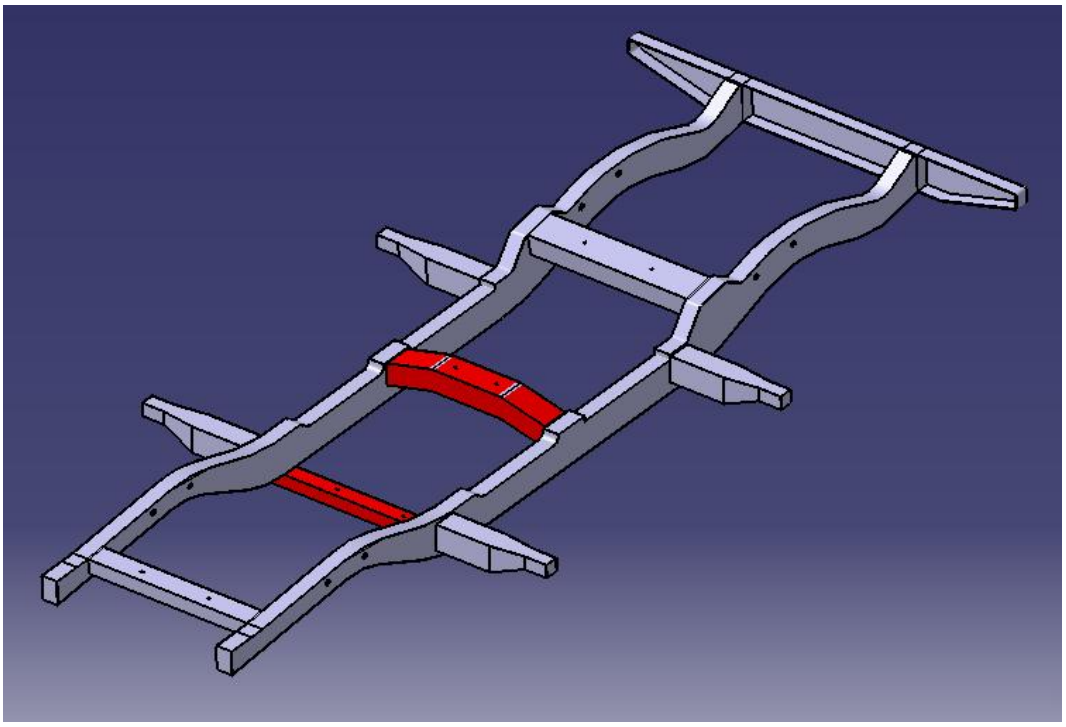

Figure 3.4: "C-model" design.

3.2.2 Models Description

In this section, the specifications of the models will be explained by presenting one of them as a generic descriptive model for them, which will clarify how to draw the structure and present general specifications such as weight, center of gravity ...etc.

In this framework, the basic model "A-model" will be presented as a generic descriptive model. The model was drawn on the CATIA program, where it was drawn as single one part, not as assembly product. The first sketch was the longitudinal-section of one of the main bridges and then a third dimension was given by a "pad" command in the program. Figure (3.5) illustrates the sketch of the longitudinal-section of the main bridge on the part design sketcher in CATIA program, where the lines and curves of the bridge are clearly obvious. The entire bridge is then reflected around the chassis symmetry axis, which is the longitudinal center axis that equalize the structure, by mirrored command in the program to form the two main bridges of the structure.

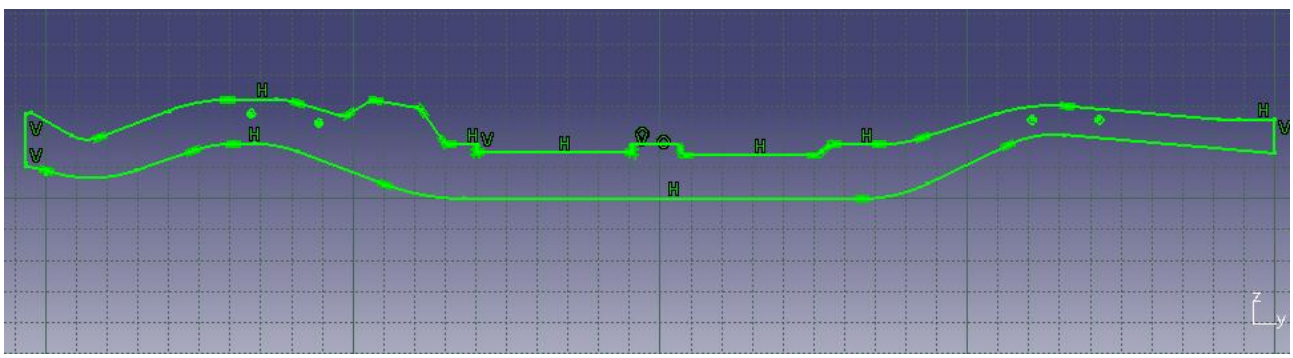

Figure 3.5: The sketch of the main bridge longitudinal-section.

After that, the sketch of cross-bridges was drawn between the two main bridges and given a third dimension to connect these bridges to each other by reaching the next main bridge. Figure (3.6) represents the cross-sectional sketch for cross-bridges and the position of it to the structure. Then, the rear bumper was sketching on the back of the two main bridges at the end of the chassis. Figure (3.7) shows the sketch of the rear bumper and its location to the chassis structure.

The body of the vehicle is connected to the chassis through four carriers, which directly connected to the main bridges as shown in figure (3.2), but these carriers are not considered as one of the main research objectives.

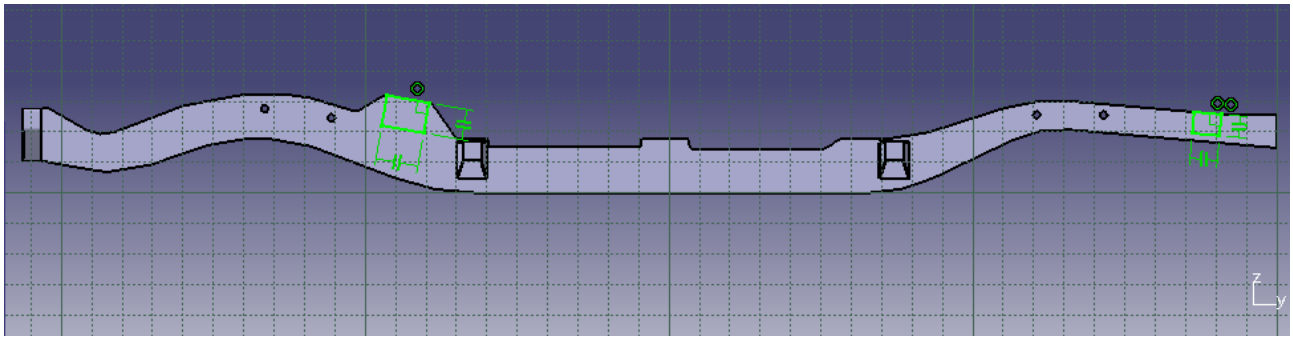

Figure 3.6: The cross-sectional sketch for cross-bridges.

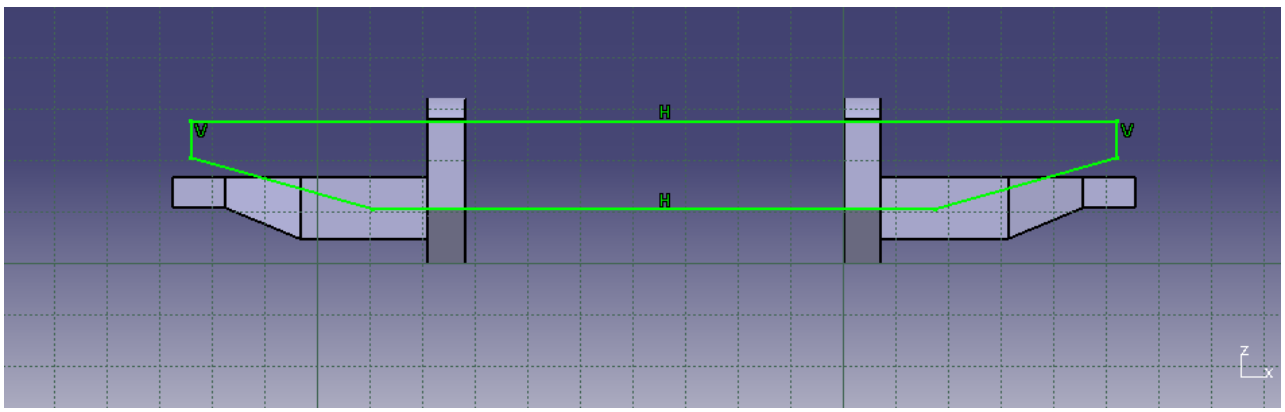

Figure 3.7: The Rear bumper sketch.

The modeling chassis is for a 4-WD, five-door Off-Road Vehicle, with a structure length of (4.13) meters, a width of (1.74) meters, and a height of no more than (0.33) meters between the lowest and highest points in the structure. The CATIA program can also gives a many characteristics information of the structure, which depend on the structural shape, dimensions, geometric distribution and the type of material. Figure (3.8) shows some of the characteristics information for the entire chassis structure.

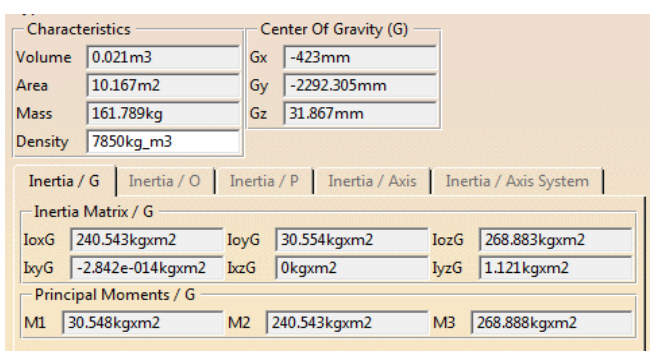

Figure 3.8: Defender chassis characteristics information.

3.3 Simulation Methodology

In the framework of achieving the research objectives, the chassis of the Defender was subjected into frontal-impact simulation tests, vehicles usually impact a solid concrete wall at a specified speed in real impacting tests as shown in figure (3.9), to examine the impact effect of the collision on the structure of the chassis and study the effect of the added cross-bridges at the durability of the chassis.

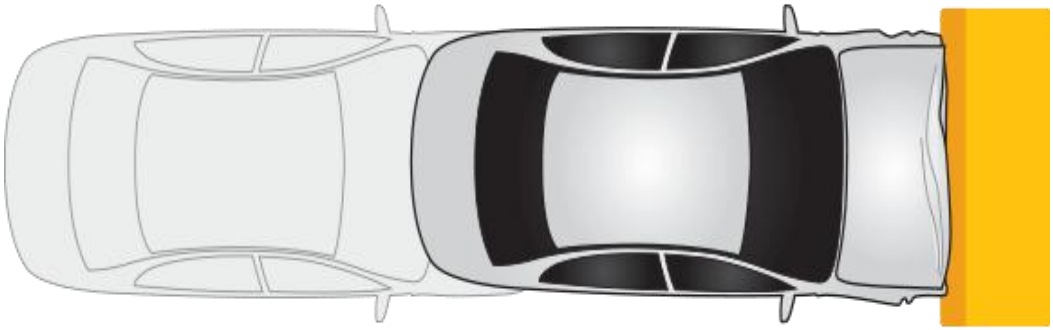

Figure 3.9: Frontal impact test description.

The chassis structure collides on a concrete wall at different speeds, in order to study the effect of the addition cross-bridges to the chassis with increasing the speed of the vehicle. The weight of other vehicle parts (as engine, drive train, wheels, driving compartment and other vehicle parts) are negligible, where the comparison between the three models meets the same conditions and criteria. Figure (3.10) shows the location of the chassis to the wall, where the wall is fixed as the chassis moving to hit it.

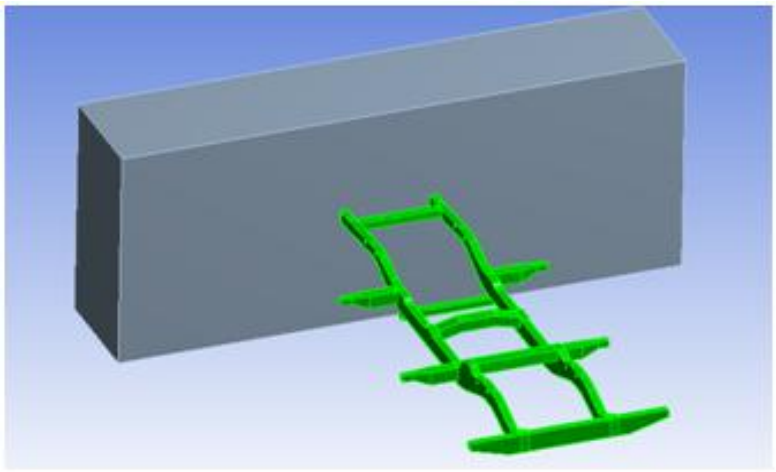

Figure 3.10: Chassis to the concrete wall view.

To implement this methodology, the ANSYS program and Explicit dynamic analysis system were used to analyze the crash tests simulation system. The following procedures explain the method that used in this research to achieve the expected collision tests. Firstly, the version of ANSYS program that used to apply the methodology is (R17.0), where figure (3.11) shows the program's interface and the version number.

Figure 3.11: ANSYS program interface.

After opening the program, the appropriate analytical system (Explicit dynamic) was selected from the toolbox and included in the schematic interface as shown in Figure (3.12). The list of materials that will be used in the simulation system is determined by the engineering data interface, as shown in figure (3.13), where the type of material and its physical properties are determined and new material can be added with new properties other than those stored within the program.

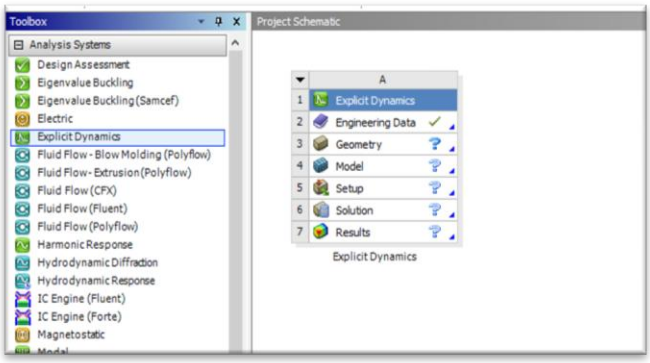

Figure 3.12: Toolbox and project schematic interface.

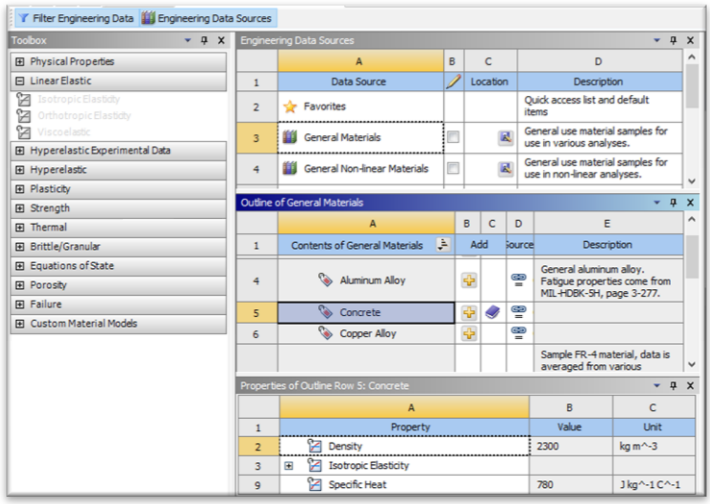

Figure 3.13: Engineering data interface.

Table (3.1) shows the characteristics of the chassis and wall materials, which are taken in ANSYS program consideration.

Table 3.1: Chassis and Wall material characteristic.

Material	Structural Steel	Concrete
Density of material (*Kg/m^3*)	7850	2300
Young's Modulus of Elasticity (*GPa*)	200	30
Poisson’s ratio	0.3	0.18

After selecting the engineering data, the geometrical process begins. The chassis structure, which drawing in the CATIA program, is imported into the ANSYS program with (igs) format for the drawing file form. Figure (3.14) shows the methods for importing the model file into the ANSYS program. After that, the geometry interface is opened to draw the concrete wall. The drawing process is starting with selecting a plane to draw the wall sketch, where the horizontal model plane is the desired plane to draw the sketch to stand against the chassis, a rectangular cross-sectional sketch, with (0.01) meter far away from the chassis to be careful not to lose energy from the system during the movement before the moment of collision. Figure (3.15) shows the wall sketch with its geometrical dimensions, this sketch is then selected to have a third dimension through the "Extrude"

command on the interface of the program. Figure (3.16) shows the standing concrete wall against the chassis with its cross-sectional sketch.

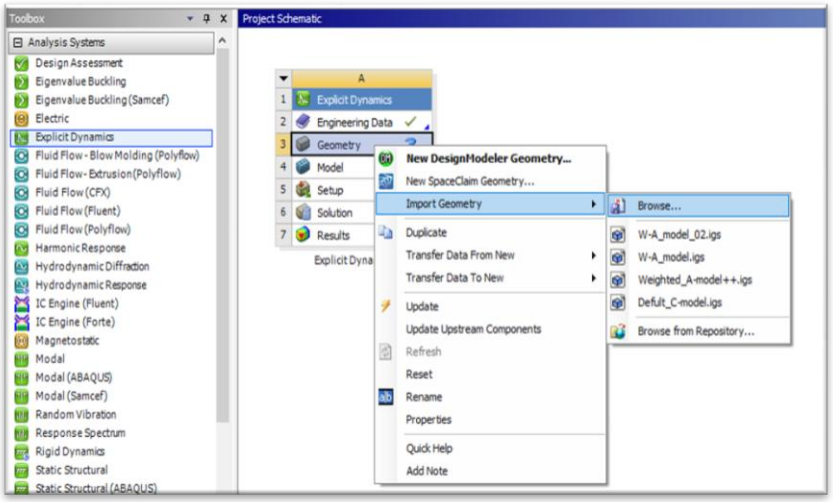

Figure 3.14: The modeling files importing methods.

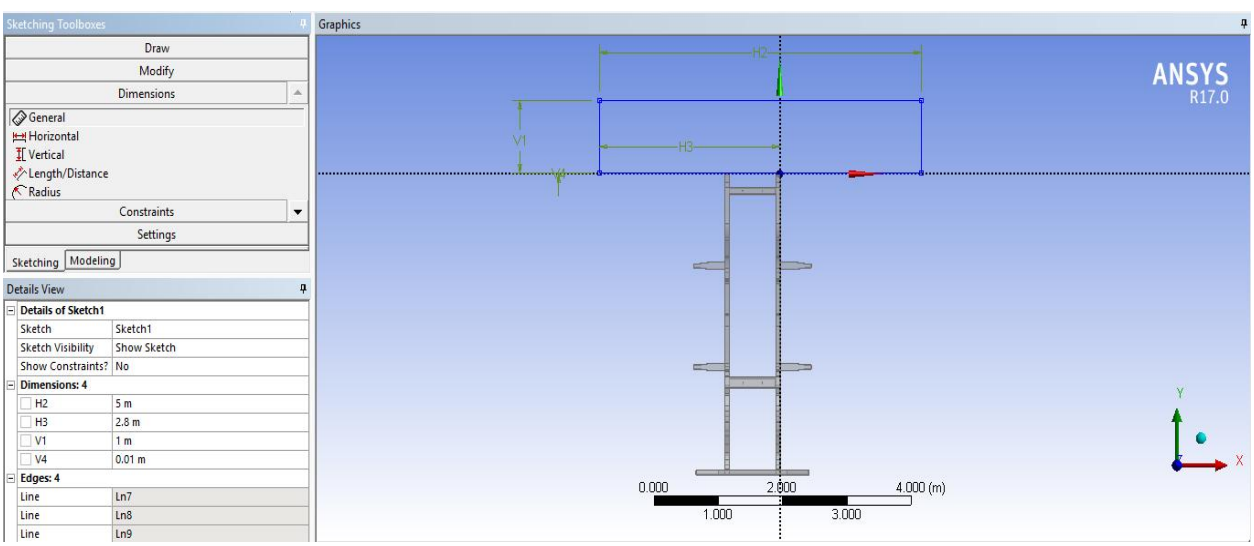

Figure 3.15: The wall sketch with geometrical dimensions.

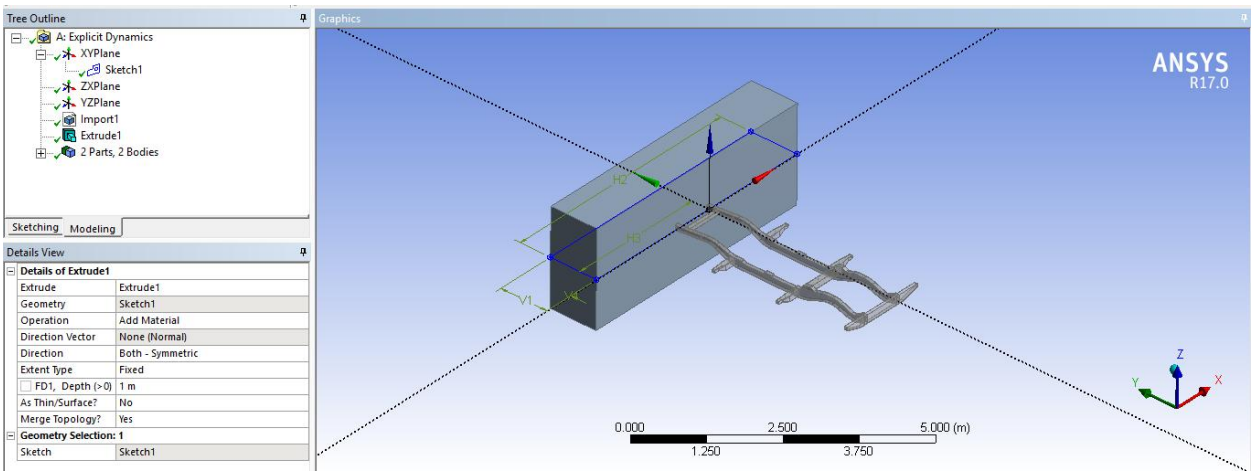

Figure 3.16: The concrete wall with its cross-sectional sketch.

To start the simulation, the modeling is selected from the project list to determine the pre-processing information and to apply the simulation process, the results can also be shown from this interface. The first procedure to be carried out for the implementation is the model discretization process according to the principle of finite element method (FEM) by the "mesh" command from the tree outline, figure (3.17) shows how the model discretization works and the meshing shape on the model. After this, the pre-processing information is start to identify for the research simulation process, the concrete wall will be fixed with a "fixed support" feature in the program, where the back face of the wall will be fixed to facing the movement of the chassis towards it, figure (3.18) shows the wall back face as a static fixed support in the system.

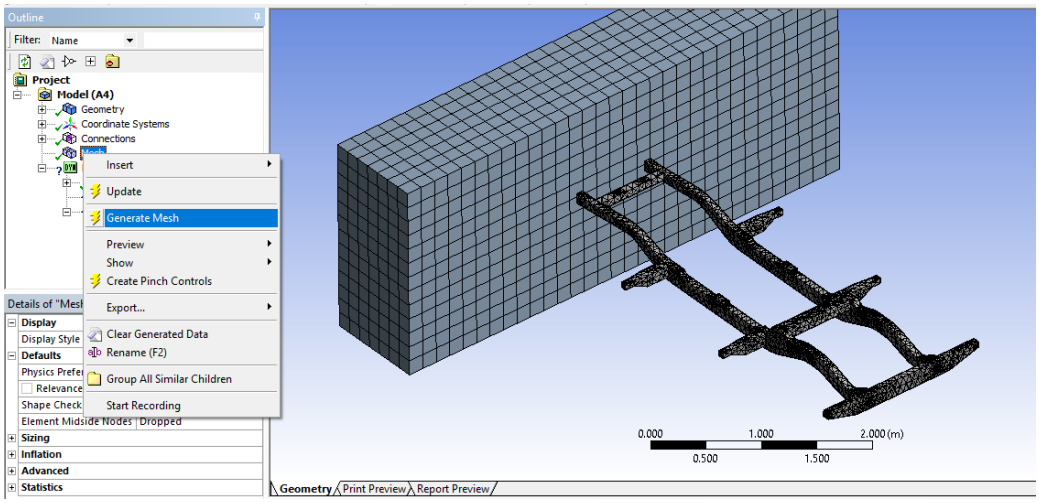

Figure 3.17: Discretization process with the meshing shape on the model.

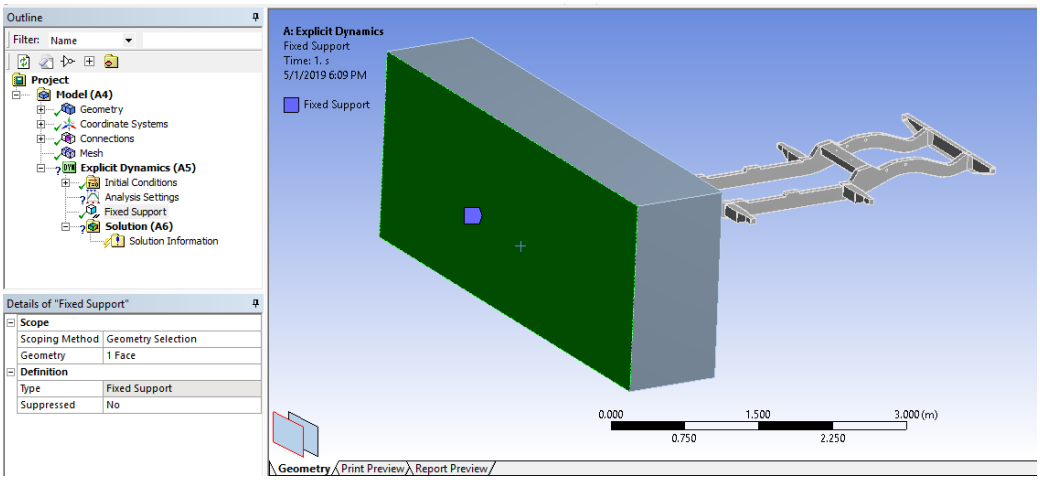

Figure 3.18: The back face of the wall as a static fixed support.

The next step is identifying the solution processing information by determining the velocity of the chassis structure, which worked as an initial condition in the simulation process. Figure (3.19) describes how to determine the velocity of the structure and its value, where the velocity direction will be in the desired movement direction of the structure. The solution process is then performed by executing the simulation solving process, by choosing a "solve" command in the interface of the program. The types of solution information, which were obtained as a result of the simulation solving process, can be determined in the postprocessor procedures by selecting its type before or after the solution process, figure (3.20) shows how to select an equivalent (Von-Mises) stress as a result of the simulation process. Also, figure (3.21) shows how to define a single point as an observation point for the stress values, where the results are either for the model in general or a specific part or area that can be identified to monitor the results.

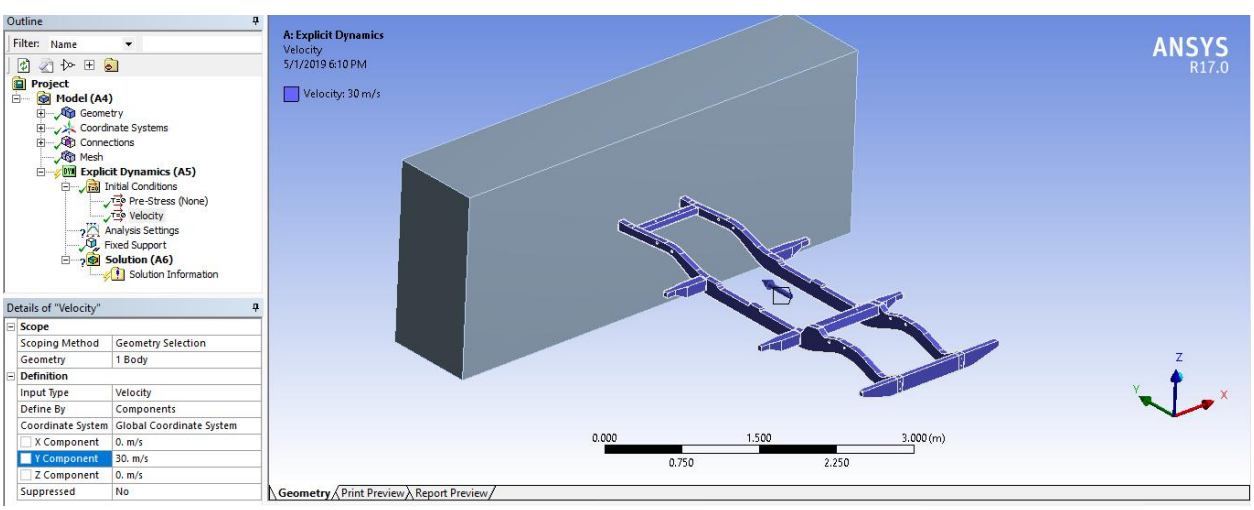

Figure 3.19: The chassis velocity determination.

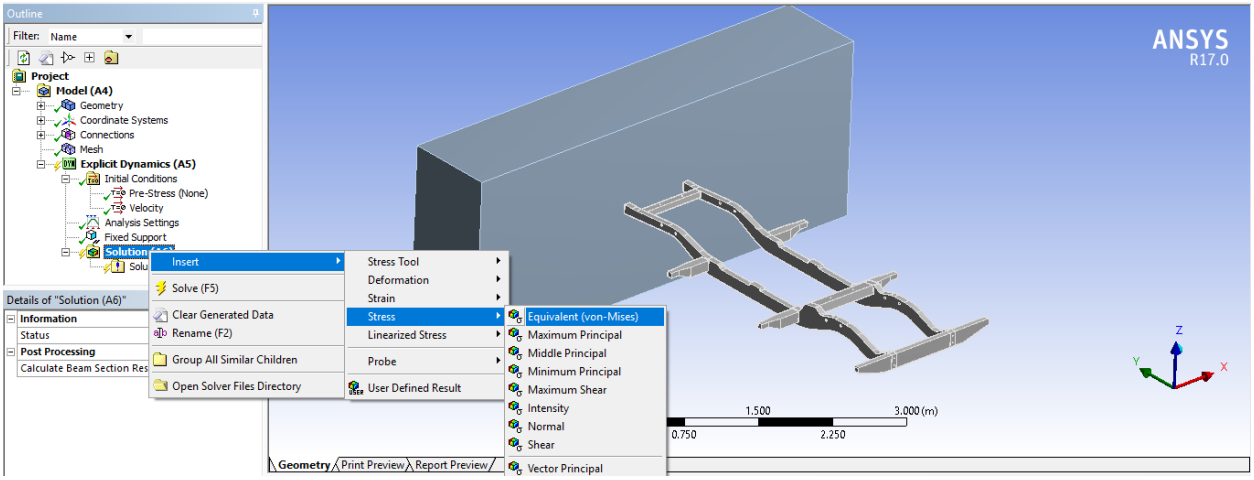

Figure 3.20: The inserting method of the solution process results.

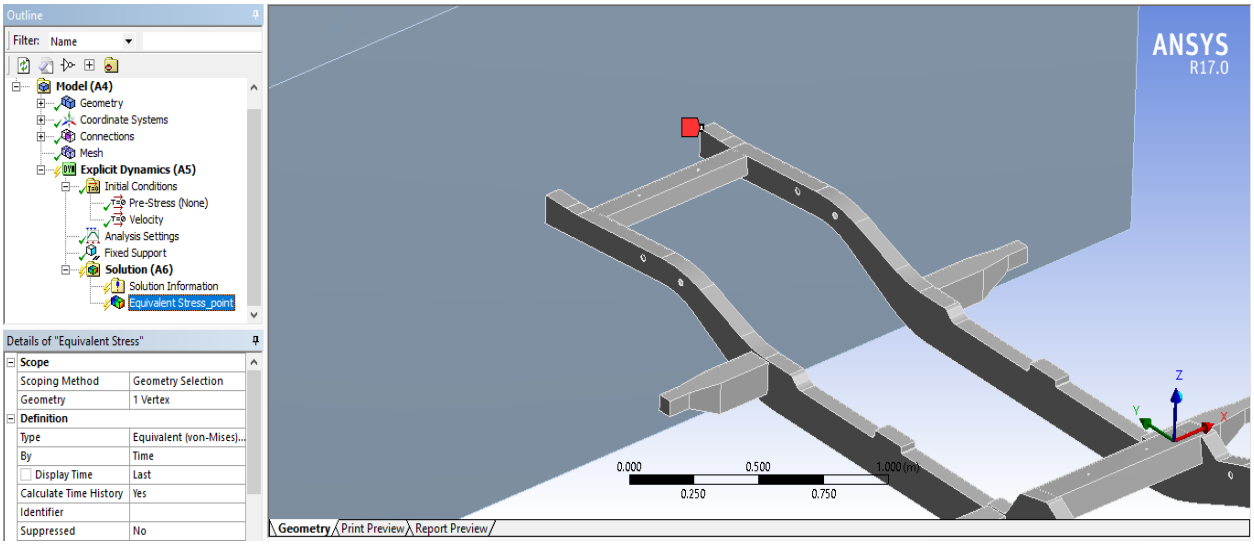

Figure 3.21: The common results observation point determination.

Figure (3.22) shows a sampling result of stress at that specified point for the "A-model" design, over the entire simulation time. The methods of displaying the results in the postprocessor are shown in the form of curve, video, chromatic gradient scale or by general report of the whole process.

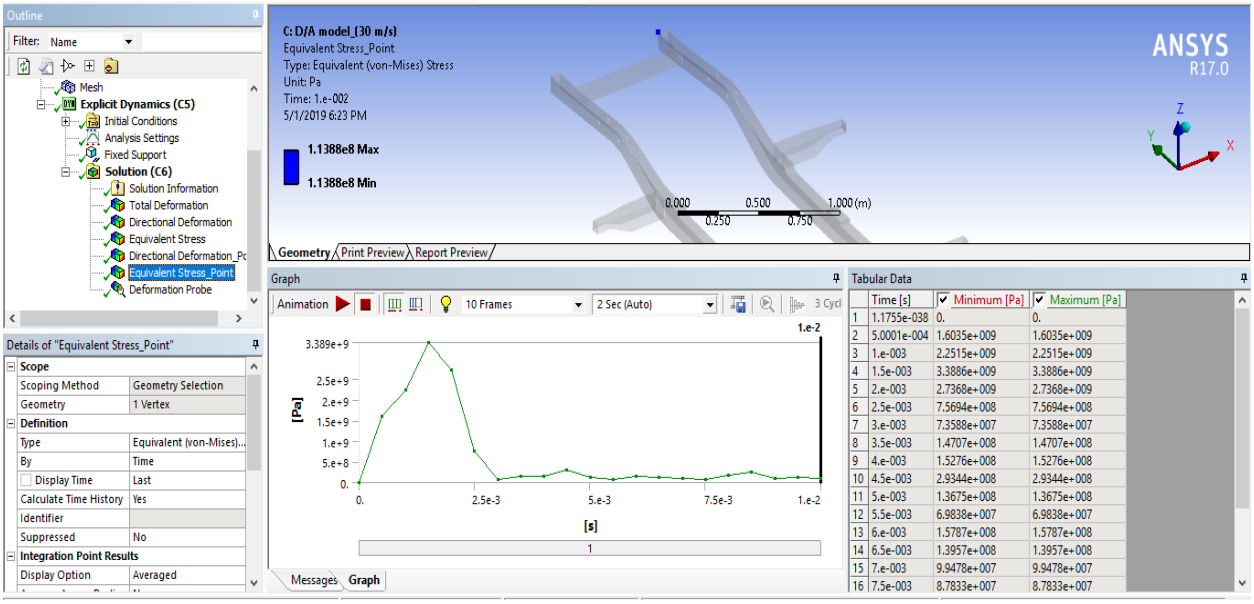

Figure 3.22: The sampling result of stress for the "A-model" design.

3.4 Results Clarification

In order to develop any model, whether for the structure of the chassis or for the vehicle in general, there must be a set of engineering results in the hands of the designers to build the design hypotheses, where basing on that results the designers were using it to find the improvements or positive developments of the model. In this context, this research aims to find such information as the values of deformation and stresses due to the effect of the cross-bridges on a range of velocities up to (200 *Km/h*), in order to use these results as an engineering tool that instructs the designers to impose the engineering hypotheses for the modifications and to examine their hypotheses at the same way.

3.4.1 Simulation Results

The simulations examined the effect of the collision into the Defender chassis, and then examined the effect of the collision on the same chassis modified by the addition of some cross-bridges to it. The first model was the "A-model" with (161.8 *Kg*) weight, while the second model "B-model" with the addition of a single cross-bridge have a weight of (168.58 *Kg*) and the latest

model "C-model" have a weight of (178.8 *Kg*), a model with two middle cross-bridges added to the basic chassis. The total deflection and stress values of the three models are taken from the same observation point, to compare the results between them under the effect of increasing the speed of the chassis during the collisions. Figure (3.21) shows the common point between the three models, which is the upper corner of the front of the chassis from its right main bridge.

Figure (3.23) shows the comparison between the three models in terms of the maximum total deflection values with increasing in the chassis collision speeds. It is noticeable from the figure that the deflection values of the front of the chassis structure, the area that collides directly to the concrete wall, began to differ between the three models after exceeding a speed of (100 *km/h*), the results were almost identical at the lower speeds and then began to vary after this speed. The first model "A-model" was the model with the least amount of deflections at high speeds, while the second model "B-model" was the model with highest deflection values at high speeds. The third model was closer to the second model in terms of deflection values at high speeds, but still the lower one.

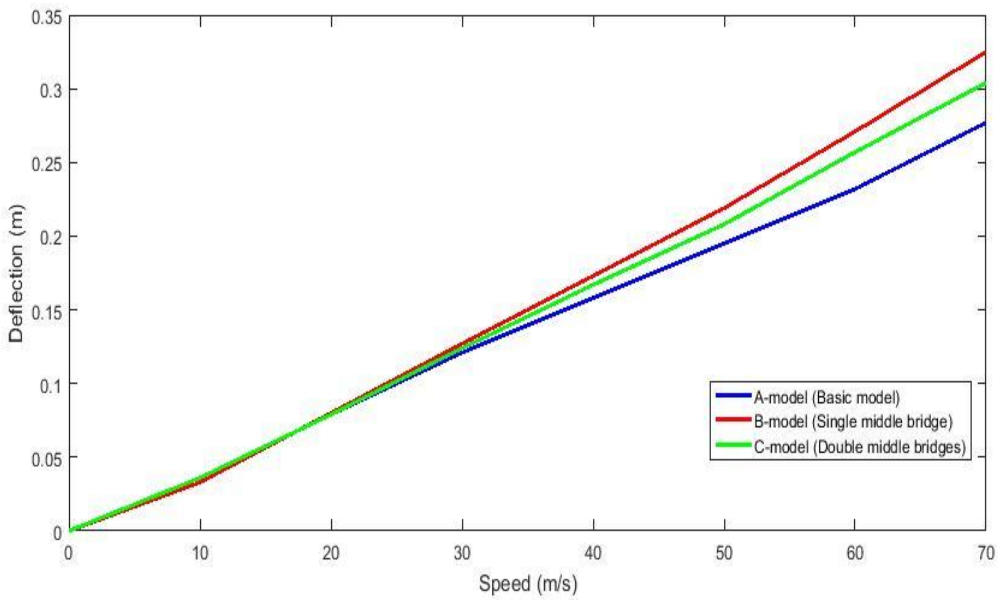

Figure 3.23: Total deflection values for three models due to increasing of speed.

Figure (3.24) shows the comparison between the three models in terms of the maximum equivalent von-mises stress values with increasing in the chassis collision speeds. It is noticeable from the figure that the stresses values of the front of the chassis structure began to differ between the three models after exceeding a speed of (140 *km/h*), the results were almost the same at the lower speeds and then began to vary after this speed. Suddenly, that the first model "A-model" was the model

with the highest values of stresses at high speeds, comparing to its level in deflection curves, while the second model "B-model" was the model with lowest values at high speeds. The third model was closer to the second model in terms of stress values at high speeds, but still the higher one. It is also noticeable that at high collision speeds, the order of models has reversed between the lowest and highest in terms of deflection and stresses values.

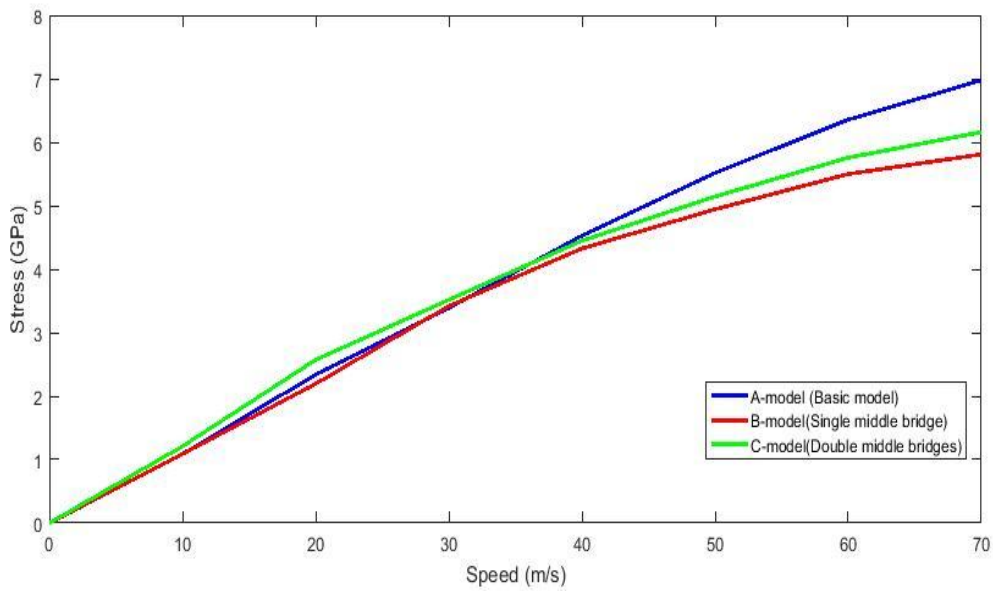

Figure 3.24: Equivalent von-mises stress values for three models due to increasing of speed.

In the context of knowledge of the behavior of the chassis material, structural steel, under the influence of collision impulse forces and high stresses values, the stress-strain curve should be defined in this case. Figure (3.25) shows the stress-strain curves at the observation point for three the models by drawing the relationship between the equivalent von-mises stress values and the equivalent von-mises strain values, which they observed in the same point. The curves of the strain values were quite identical in shape to the stress values curves, in terms of increasing its values due to speed and the models ordering also, which obviously clear in resulting straight lines of the stress-strain curves, Fig. (3.25).

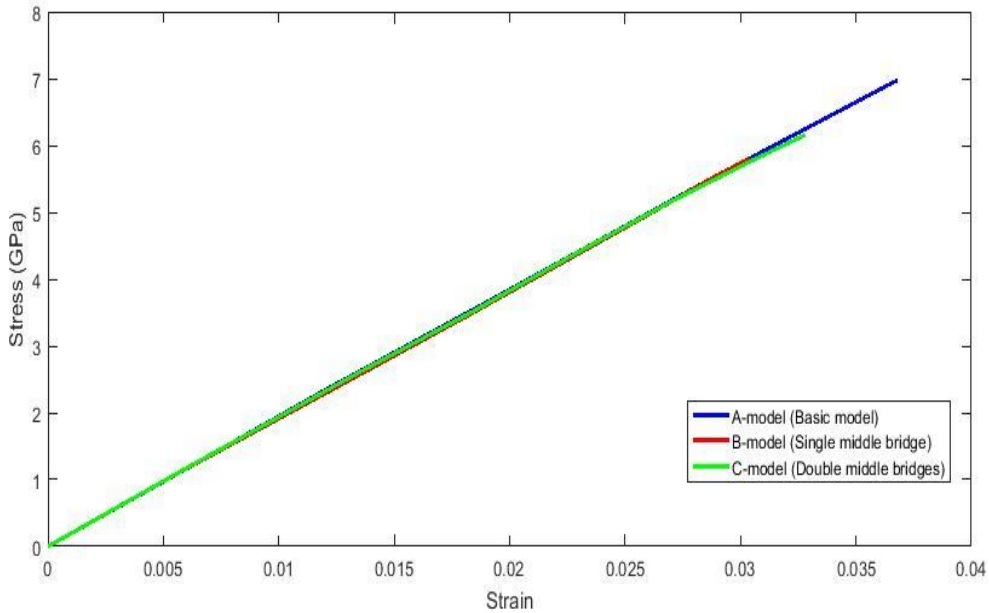

Figure 3.25: The stress-strain curves for the three models at the observation point.

3.4.2 Results Discussion

As noted from the previous results, especially the stresses diagram, Fig. (3.24), that the models having intermediate bridges added to the chassis structure gives a less values of stress comparing with the basic model at the same accident conditions. The addition of cross-bridges reduces the stress values at the front of the chassis depending on their shapes and positions in the structure. The function of the cross-bridge, as shown here, is to divide the strain energy generated by collisions that discharges into the structure by finding new paths for forces to flow on it, where its effect will be reduced on other structure bridges.

Figure (3.23) shows the maximum total deflections diagram for the front of the chassis at the end of the specified collision duration in the program during simulations, which is (10) milliseconds due to the large time needed in solving processes, which are not the total and final deformation of the chassises after the accident is fully end. It is noticeable from figure (3.25) that the behavior of the chassis material does not exceed the linear elastic limit. Therefore, these values of deflection will be zero, without any noticeable permanent strain, if the applying duration of the solving process is big enough. The (10 *msec*) duration period is considered suitable for studying the shock impact effects

and observing the stresses maximum values on the structure. Figure (3.22) shows a sampling stress behavior represented at (2.5 *msec*), which is a quarter of the collision specified duration.

From the above, these results are not sufficient to describe the total effect of the collision on the entire structure of the vehicle chassis, also they are not sufficient to determine the actual effect of the additional cross-bridges in terms of its different positions that located in the chassis structure. This weakness is due to the fact that the results were monitored, or observed, from one single location only. To have a full knowledge for the total collision effect on the structure, a many observing points distributed on the entire structure must be use or by constructing a full path that describes all components of the structure, which will be the observation path of the study.

4

Chapter Four

Project Conclusion and Recommendations

4.1 Project General Conclusion.

4.2 Recommendations.

4.1 Project General Conclusion

This project aims to study the structural design of a vehicle chassis, in order to use its analytical results to reconstructing an improved structure according to the standards of engineering design and international environmental institutions.

This book presents in its contents a detailed presentation of a graduation project entitled (Simulation and Analysis of a Vehicle Chassis by ANSYS Program) to obtain a bachelor's degree in mechanical engineering. The book presents in its first chapter an introduction of the project and its ideas, objectives, challenges and motivations that prompted researchers to research in this subject. It also presents what other researchers have done in similar fields. At the end of the first chapter, the book shows the times-tasks distribution on the project duration over two semesters from the date of start to finish.

Then, the book presents, in the first part of its second chapter, an introduction to the theory of the analytical analysis method that used in the project, as well as a general description of the engineering analysis program (ANSYS). After that, the book presents an explanation of the appropriate analysis system for the research, in terms of its applications and its solution methodology for the engineering problems as well as the mathematical theory of the system. In the second part, of the same chapter, the book presents a scientific background on the physical theories of the research, by clarifying a set of engineering scientific topics that describe the project procedure.

Finally, the book presents in the third chapter a general description of the structure of the vehicle chassis, that represented in simulations, and for the chassis models that were drawn by the CATIA program, where the models drawing methodology is also presented and how to create a simulation system on the ANSYS program. At the end of the chapter, the book presents the research results by showing a series of diagrams that describes the behavior of the structure during the collision, and presents the explanations of these results based on the scientific background presented in the second chapter. The book fourth chapter presents a general description of its contents, as well as the recommendations proposed by the Project team as secondary outcomes.

4.2 Recommendations

This research was presented mainly to the idea of design and developing automotive chassis by testing them into crash test simulations. In this context, the research team presented a set of scientific recommendations to develop their project as a result of what they learned and discovered in the framework of their research. The most important of these recommendations are:

- As explained earlier, this research has a weakness on its results, due to the lacks of descriptive results for the chassis structure. Therefore, extraction a many of the descriptive results by spreading the results monitoring points is the best step to obtain more comprehensive results to describe the behavior of the chassis during accidents.

- In this research, to study the behavior of the chassis during the collision, the weight of the passenger compartment has been completely neglected. However, the addition of the weight of the cabin will help to better represent for the effect of the impact on the vehicle, for both its body and chassis.

- This study presents the effect of collision on the chassis by subjecting it to the simulating frontal car crash test. Therefore, the simulating of other versions of the vehicle collisions (like: side impact test, driver-side impact test, roll-over test...etc.) will give a More comprehensive results to the effect of chassis structural design during the accidents.

- The chassis was represented in this research as a structure with single consisting material, structural steel, but studying the effect of using multiple materials in chassis structural design is one of the largest researching areas in the car developments fields, recently in the world.

References

1. Patel Vijaykumar, V. and R. Patel, *Structural analysis of automotive chassis frame and design modification for weight reduction.* International Journal of Engineering Research & Technology, 2012.

2. S. S. Sane, G.J., Anandraj H., "*Stress Analysis of a Light Commercial Vehicle Chassis by FEM*".

3. Cavazzuti, M., et al., *Structural Optimization of Automotive Chassis: Theory, Setup, Design*. Structural and Multidisciplinary Optimization, 2011.

4. Chandra, M.R., S. Sreenivasulu, and S.A. Hussain, *Modeling and Structural analysis of heavy vehicle chassis made of polymeric composite material by three different cross sections*. International Journal of Modern Engineering Research, 2012.

5. Patil, H.B., S.D. Kachave, and E.R. Deore, *Stress analysis of automotive chassis with various thicknesses.* IOSR Journal of Mechanical and Civil Engineering, 2013.

6. Patel, H., K.C. Panchal, and C.S. Jadav, *Structural analysis of truck chassis frame and design optimization for weight reduction*. International Journal of Engineering and Advanced Technology, 2013.

7. Reddy, M.M. and L.K. Reddy, *Modeling and Analysis of container chassis using FEM*. International Organization of Scientific Research Journal of Engineering (IOSRJEN), 2014.

8. Swami, K. and S. Tuljapure, *Analysis of Ladder Chassis of Eicher 20.16 Using FEM*. IOSR Journal of Applied Geology and Geophysics (IOSR-JAGG), 2014.

9. ANSYS Workbench Program, "*help*" list, *Mechanical applications*, *Explicit dynamics analysis guide overview.*

10. Meriam, J.L. and L.G. Kraige, *Engineering mechanics*: dynamics. Vol. 2. 2012: John Wiley & Sons.

11. Gere, J.M., *Mechanics of Materials*. 2004. 6th Edition.